NIPE Núcleo de Investigação em Políticas Económicas e Empresariais

#12
2021

WORKING PAPER

Susana Campos-Martins
Cristina Amado

"Modelling Time-Varying Volatility Interactions"

https://nipe.eeg.uminho.pt/

FCT Fundação para a Ciência e a Tecnologia

«This paper is financed by National Funds of the FCT – Portuguese Foundation for Science and Technology within the project «UIDB/03182/2020»

Universidade do Minho
Escola de Economia e Gestão

Modelling Time-Varying Volatility Interactions

Susana Campos-Martins*
University of Oxford
University of Minho and NIPE

Cristina Amado†
University of Minho and NIPE
CREATES and Aarhus University

September 08, 2021

Abstract

In this paper, we propose an additive time-varying (or partially time-varying) multivariate model of volatility, where a time-dependent component is added to the extended vector GARCH process for modelling the dynamics of volatility interactions. In our framework, co-dependence in volatility is allowed to change smoothly between two extreme states and second-moment interdependence is identified from these crisis-contingent structural changes. The estimation of the new time-varying vector GARCH process is simplified using an equation-by-equation estimator for the volatility equations in the first step, and estimating the correlation matrix in the second step. A new Lagrange multiplier test is derived for testing the null hypothesis of constancy co-dependence volatility against a smoothly time-varying interdependence between financial markets. The test appears to be a useful statistical tool for evaluating the adequacy of GARCH equations by testing the presence of significant changes in cross-market volatility transmissions. Monte Carlo simulation experiments show that the test statistic has satisfactory empirical properties in finite samples. An application to sovereign bond yield returns illustrates the modelling strategy of the new specification.

JEL classification codes: C12, C13, C32, C51, G15.
Keywords: Multivariate time-varying GARCH; Volatility spillovers; Time-variation; Lagrange multiplier test; Financial market interdependence.

*Nuffield College, University of Oxford, 1 New Road, Oxford OX1, United Kingdom; e-mail address: susana.martins@nuffield.ox.ac.uk.

†Corresponding author: Department of Economics and NIPE, University of Minho, Campus de Gualtar, 4710-057 Braga, Portugal; e-mail address: camado@eeg.uminho.pt.

1 Introduction

The class of conditional correlation (CC-)GARCH models of financial time series has become a standard tool for modelling and forecasting correlations between financial returns. Following the constant conditional correlation (CCC-)GARCH model of Bollerslev (1990) many parametric extensions have been proposed in the literature on building more flexible models for describing time-varying conditional correlations. The models introduced by Tse and Tsui (2002) and Engle (2002) with dynamic conditional correlations postulating a GARCH-type dynamics on the correlations have become particularly popular among practitioners. For surveys about these and other multivariate GARCH models, see Bauwens et al. (2006) and Silvennoinen and Teräsvirta (2009).

As a result of financial market connectivity, the analysis of interdependence and interactions in volatility is also useful to earn knowledge on how information is transmitted across markets. Understanding the transmission mechanism of financial market movements is important for portfolio risk management and for successful hedging and trading strategies. A large number of studies have documented evidence of interdependence and linkages across financial markets or assets. Empirical studies providing evidence for volatility spillovers include Baillie and Bollerslev (1990), King and Wadhwani (1990), Hamao et al. (1990), Lin et al. (1994), Cheung and Ng (1996), Forbes and Rigobon (2002), Cifarelli and Paladino (2005), among others.

Despite the extensive literature investigating co-movements between financial markets, most of research has been focused on the interdependence in terms of the conditional first moments of the distribution of returns, and less attention has been devoted to exploring financial interactions in terms of the second moments. A few examples of the former include Diebold and Yilmaz (2009) who used vector autoregressive methods for examining the transmission of financial market movements. Chiang and Wang (2011) proposed an autoregressive range-based volatility model and employed a smooth transition copula function to further examine financial volatility contagion between financial stock markets of the G7 countries. Leung et al. (2017) used a linear regression approach to study volatility spillovers (or interactions) between the GARCH volatilities of equity and exchange rate markets to equity markets during periods of financial crises. Yet, the findings in Engle and Susmel (1993)

and Diebold and Yilmaz (2009) suggest that cross-market volatility interactions convey more insightful information about the dynamics of co-movements across markets than linkages in returns.

Several specification techniques have been employed in the literature for examining the dynamics of financial market interdependence, but few attempts to investigating time-varying volatility transmission mechanism spillovers exist in the literature. An interesting extension that builds on the assumption of time-invariant correlations in an attempt to capture volatility spillovers was suggested by Jeantheau (1998) generalizing the diagonal CCC-GARCH model to the so-called extended (E)CCC-GARCH model wherein dynamic volatility interactions between markets are allowed in the form of cross-market ARCH and GARCH effects. Yet recent research found evidence of time-variation and structural shifts in the transmission mechanisms of shocks to volatility during periods of financial market distress. Examples documenting time-varying volatility spillovers can be found in Karanasos et al. (2014), Jung and Maderitsch (2014), Karanasos et al. (2018) and Liu and Gong (2020).

While the class of conditional correlation GARCH models has been extensively employed for quantifying and examining volatility transmission mechanism spillovers, less attention has been addressed to the misspecification of the GARCH structure of these models, and the contribution of this paper lies in that direction. Testing the assumption of constant volatility spillovers between time series is an important specification tool for building multivariate GARCH models. Modelling volatility spillovers would be only relevant when the null hypothesis of no interactions is rejected. For a comprehensive discussion of tests for volatility spillovers see, for example, Hong (2001), Nakatani and Teräsvirta (2009) and Pedersen (2017). Other specification issues of interest include alleviating the curse of dimensionality in large systems or developing models whose parametric structure is well suited for time-varying co-movements across markets.

This paper contains two novelties. First, we propose a novel extension of the ECCC-GARCH representation of Jeantheau (1998) suited to model time-varying conditional variances and cross-market volatility interactions. It is based on decomposing additively the conditional variance equations into two components, one describing clustering volatility specified as a measurable function of the past of all elements of the vector of returns, and

another representing the misspecification of the volatility structure. One type of model misspecification includes omitting a time-dependent component to the extended vector GARCH model in the form of structural changes in the volatility process. Other types of model misspecification in the functional form of the conditional variances could also be considered. Second, we introduce statistical tests based on the Lagrange multiplier principle as an useful validation tools to reveal against such type of model misspecification. Monte Carlo simulations show that the tests have reasonable good size and power in finite samples.

Our modelling strategy relies on by first testing the adequacy of the specification against the alternative of the additive time-dependent vector GARCH model and estimating such nonlinear extension only in case of rejection of the null hypothesis. For numerical simplicity, we shall adopt the two-step estimation approach proposed by Francq and Zakoïan (2016) where the univariate conditional variances are estimated equation-by-equation in the first step and the conditional correlations are estimated in the second step conditionally on the first step estimates. Finally, we shall illustrate our modelling cycle with an application to study the dynamics of the co-movements among bond yield returns on the 10-year government Greek, Irish and Portuguese sovereign markets.

The remaining sections of this paper are organised as follows. Section 2 introduces the new model and its properties. In Section 3 is discussed the equation-by-equation estimation of parameters and the asymptotic properties of the quasi-maximum likelihood estimator (QMLE). Section 4 is devoted to Lagrange multiplier tests for time-varying volatility interactions. Section 5 presents some evidence of the small sample properties of the statistical tests by Monte Carlo simulations. In Section 6 we illustrate the functioning of the modelling strategy to sovereign bond yield returns. Finally, Section 7 concludes the paper.

2 The model and assumptions

Consider the observable stochastic $m-$dimensional vector of returns

$$\boldsymbol{\varepsilon}_t = \boldsymbol{\Sigma}_t^{1/2}\mathbf{z}_t, \qquad t = 1, ..., T, \tag{1}$$

where the stochastic vector $\mathbf{z}_t = (z_{1t}, ..., z_{mt})'$ is a sequence of independent random variables with $\mathsf{E}\mathbf{z}_t = \mathbf{0}$ and a time-varying positive definite correlation matrix $\mathsf{E}\mathbf{z}_t\mathbf{z}_t' = \mathbf{P}_t = [\rho_{ij,t}]$, such that $\rho_{ii,t} = 1$ and $\rho_{ij,t} \neq 0$, $i, j = 1, ..., m$. It follows that the error vector $\boldsymbol{\zeta}_t = \mathbf{P}_t^{-1/2}\mathbf{z}_t \sim$ iid$(\mathbf{0}, \mathbf{I}_m)$, where $\mathbf{I}_m$ is the $m \times m$ identity matrix. Without loss of generality, we assume the conditional mean of the vector of returns to be equal to zero. With these assumptions, the vector process $\boldsymbol{\varepsilon}_t$ is a martingale-difference

$$\mathsf{E}(\boldsymbol{\varepsilon}_t|\mathcal{F}_{t-1}) = \mathbf{0} \tag{2}$$

with a symmetric conditional covariance matrix defined as

$$\mathsf{E}(\boldsymbol{\varepsilon}_t\boldsymbol{\varepsilon}_t'|\mathcal{F}_{t-1}) = \boldsymbol{\Sigma}_t \tag{3}$$

where $\mathcal{F}_{t-1}$ is the $\sigma-$algebra generated by the past information about $\boldsymbol{\varepsilon}_t$ available at time $t-1$. The conditional covariance matrix $\boldsymbol{\Sigma}_t = [\sigma_{ij,t}]$ is assumed to be multiplicatively decomposed in the usual fashion:

$$\boldsymbol{\Sigma}_t = \mathbf{D}(t/T)\mathbf{P}_t\mathbf{D}(t/T) \tag{4}$$

where T is the sample size and $\mathbf{D}(t/T) = \mathsf{diag}(\sigma_1(t/T), \ldots, \sigma_m(t/T))$ is a diagonal matrix of conditional standard deviations of the process $\boldsymbol{\varepsilon}_t$. Each component $\sigma_i(t/T)$, $i = 1, ..., m$, is a smooth time-dependent function describing structural changes in the conditional variance.

In this paper, we generalise the class of conditional correlation GARCH models by introducing nonstationarity in the own-market volatility process and cross-market volatility interactions. We shall rely on statistical inference to specify the most appropriate parameterization of $\sigma_i^2(t/T)$ so that it captures completely the past information. More details about the statistical test shall be discussed in Section 4. We assume that $\boldsymbol{\sigma}_t^2 = (\sigma_{1t}^2, ..., \sigma_{mt}^2)'$ is defined as a time-varying representation measurable with respect to $\mathcal{F}_{t-1}$ with the additive decomposition:

$$\boldsymbol{\sigma}_t^2 = \mathbf{h}_t + \mathbf{g}_t \tag{5}$$

where $\mathbf{h}_t$ is the stationary component allowing for volatility interactions across markets and

$\mathbf{g}_t$ is the time-dependent volatility component of rescaled time. This rescaling technique for the calendar time is useful for obtaining a meaningful asymptotic theory (Dahlhaus and Rao (2006)), but establishing the asymptotic properties of the maximum likelihood estimators is beyond the scope of this paper.

We assume that $\mathbf{h}_t$ is specified as the vector GARCH (p, q) process:

$$\mathbf{h}_t = \boldsymbol{\omega} + \sum_{i=1}^{q} \mathbf{A}_i \boldsymbol{\varepsilon}_{t-i}^2 + \sum_{j=1}^{p} \mathbf{B}_j \mathbf{h}_{t-j} \tag{6}$$

where $\mathbf{h}_t = (h_{1t}, ..., h_{mt})'$, $\boldsymbol{\varepsilon}_t^2 = (\varepsilon_{1t}^2, ..., \varepsilon_{mt}^2)'$, $\boldsymbol{\omega}$ is an $m \times 1$ intercept vector with strictly positive components, and $\mathbf{A}_i$ and $\mathbf{B}_j$ are $m \times m$ matrices with positive entries.

To introduce time-variation in the volatility dynamics, we define the nonstationarity component $\mathbf{g}_t$ as follows:

$$\mathbf{g}_t = \left(\boldsymbol{\omega}^* + \sum_{i=1}^{q} \mathbf{A}_i^* \boldsymbol{\varepsilon}_{t-i}^2 + \sum_{j=1}^{p} \mathbf{B}_j^* \mathbf{h}_{t-j} \right) \mathbf{G}(t/T) \tag{7}$$

where $\mathbf{g}_t = (g_{1t}, ..., g_{mt})'$ is a $m \times 1$ stochastic time-varying vector, $\boldsymbol{\omega}^*$ is an $m \times 1$ intercept vector, $\mathbf{A}_i^*$ and $\mathbf{B}_j^*$ are $m \times m$ matrices, and $\mathbf{G}(t/T) = \mathsf{diag}(G_1(t/T; \gamma_1, \mathbf{c}_1), \ldots, G_m(t/T; \gamma_m, \mathbf{c}_m))$ is a diagonal matrix of m transition functions defined below in (8). Further simplification of the model is possible by letting $\mathbf{B}_j$ to be diagonal to alleviating the computational burden and reducing the dimensionality curse without preventing the high-dimensional property of the model. In what follows, we shall assume $\mathbf{B}_j$ to be diagonal matrices while keeping the specification of the correlation matrix fairly general.

Each component of the matrix $\mathbf{G}(t/T)$ is represented by the general logistic transition function $G_i(t/T; \gamma_i, \mathbf{c}_i)$, $i = 1, ..., m$, with the form

$$G_i(t/T; \gamma_i, \mathbf{c}_i) = \left(1 + \exp\left\{ -\gamma_i \prod_{k=1}^{k_i} (t/T - c_{ik}) \right\} \right)^{-1}, \gamma_i > 0, c_{i1} \leqslant \cdots \leqslant c_{ik_i} \tag{8}$$

where $\mathbf{c}_i = (c_{i1}, \ldots, c_{ik_i})'$ is the vector of k_i location parameters. The function $G_i(t/T; \gamma_i, \mathbf{c}_i)$ is continuous for $\gamma_i < \infty$ and bounded between zero and one. By construction, when $\gamma_i = 0$ for all $i = 1, \ldots, m$, the model collapses into the augmented GARCH specification of Francq and Zakoïan (2016). The parameters $\mathbf{c}_i$ and γ_i determine the location and the speed of

transition from one state to another. For smaller values of γ_i, the changes between volatility regimes are smooth, but when $\gamma_i \to \infty$, structural breaks can be identified at $c_{ik}, k = 1, \ldots, k_i$. The dimension of $\mathbf{c}_i$ is determined by testing a sequence of nested hypothesis as in Lin and Teräsvirta (1994) and Teräsvirta (1994). Equations (1)-(8) jointly define the time-varying extended conditional correlation (TV-ECC-) GARCH model. The modelling strategy for building the TV-ECC-GARCH model is similar to the specific-to-general strategy for nonlinear models of the conditional mean considered in, among others, Teräsvirta (1998a) and Teräsvirta et al. (2010). Details shall be considered in Section B in the Supplementary Appendix.

Furthermore, we assume that the following conditions are satisfied:

Assumption 1. *The true vector of parameters* $\boldsymbol{\theta}_0 \in \boldsymbol{\Theta}$ *lies in the interior of the compact parameter space* $\boldsymbol{\Theta}$.

Assumption 2. *The log-likelihood has a unique maximum at the true parameter vector* $\boldsymbol{\theta}_0 \in \boldsymbol{\Theta}$.

Assumption 3. *The error terms* $z_{i,t} \sim iid$ *with* $E[z_{i,t}|\mathcal{F}_{t-1}] = 0$, $E[z_{i,t}^2|\mathcal{F}_{t-1}] = 1$, $i = 1, ..., m$. *In addition,* $E|z_{i,t}^{2(2+\phi)}| < \infty$ *for some* $\phi > 0$ *and* $i = 1, ..., m$.

Assumption 4. *The elements of* $\mathbf{G}(t/T)$ *satisfy* $\inf_{\boldsymbol{\tau} \in \boldsymbol{\Theta}} G_i(t/T; \gamma_i, \mathbf{c}_i) \geq G_{min} > 0$, *for* $i = 1, ..., m$.

Assumption 5. *The slope parameters and the location parameters satisfy, respectively, the identification restrictions* $\gamma_i > 0$ *and* $c_{i1} \leq \cdots \leq c_{ik_i}, i = 1, ..., m$.

Assumption 6. $\mathbf{P}_t$ *is a positive-definite correlation matrix for all* $\boldsymbol{\theta} \in \boldsymbol{\Theta}$.

Remark 1. *Assumptions 1 and 2 are standard regularity conditions. The "fourth-moment restriction" in Assumption 3 is necessary to guarantee the existence of the variance of the score. Assumption 4 is required for positivity and boundedness of the deterministic component* g_{it}, $i = 1, ..., m$. *The conditions in Assumption 5 are identification restrictions required for the existence of a unique maximum value for the log-likelihood function. Assumption 6 is needed for positive definiteness of* $\boldsymbol{\Sigma}_t$.

Many different forms of parameterizations are possible for $\mathbf{P}_t$. We shall focus on the constant correlation structure, that is, $\mathbf{P}_t = \mathbf{P}$, when deriving the misspecification test of the GARCH equations in Section 4. The above formulation nests the special case of the extended constant conditional correlation (ECCC-)GARCH model in Jeantheau (1998). The assumption of nonnegative volatility parameters is a sufficient condition for ensuring the positive definiteness of the conditional covariance matrix in this specification; for references see the Definition 3.1 in Jeantheau (1998), the Assumption 3 in Ling and McAleer (2003) and the Section 3 in Francq and Zakoïan (2012). In order to allow for negative volatility spillovers, we refer to the conditions derived in Conrad and Karanasos (2010).

A very flexible model can be obtained by letting the specification of $\mathbf{P}_t$ unspecified. An often used parsimonious specification for the correlation matrix is defined by the dynamic conditional correlation (DCC-) GARCH model of Engle (2002). Alternatively, we allow the unconditional correlations to change smoothly between two extreme states as in the smooth transition conditional correlation model of Silvennoinen and Teräsvirta (2005, 2015).

Remark 2. *Positive definiteness of* $\mathbf{\Sigma}_t$ *is ensured provided that the conditional variances* $\sigma_i^2(t/T)$ *are strictly positive and* $\mathbf{P}_t$ *is a well-behaved correlation matrix. The additional conditions that elements of* $\boldsymbol{\omega}+\boldsymbol{\omega}^*$ *are positive, and the elements of* $\mathbf{A}_i+\mathbf{A}_i^*$ *and* $\mathsf{diag}(\mathbf{B}_j+\mathbf{B}_j^*)$, $i = 1, \ldots, q$, $j = 1, \ldots, p$ *are non-negative are sufficient to guarantee* $\sigma_i^2(t/T) > 0$, *for all* i. *When these constraints are satisfied and* $\mathbf{P}_t$ *is positive definite, the matrix* $\mathbf{\Sigma}_t$ *is positive definite almost surely for all* t.

3 Equation-by-equation estimator

3.1 The log-likelihood function

We begin by introducing some notation. Let the parameter vector $\boldsymbol{\theta}$ be partitioned into $\boldsymbol{\theta} = (\boldsymbol{\vartheta}', \boldsymbol{\rho}')'$, where $\boldsymbol{\vartheta}$ denotes the volatility parameter vector and $\boldsymbol{\rho} = \text{vecl}(\mathbf{P}_t)$ is the $m(m-1)/2$-dimensional vector of correlation parameters, where the operator vecl stacks the lower off-diagonal elements of the symmetric $m \times m$ matrix $\mathbf{P}_t$. The vector $\boldsymbol{\vartheta}$ is further partitioned into $\boldsymbol{\vartheta} = (\boldsymbol{\phi}', \boldsymbol{\varphi}')'$, where $\boldsymbol{\phi} = (\boldsymbol{\phi}_1', ..., \boldsymbol{\phi}_m')'$ and $\boldsymbol{\varphi} = (\boldsymbol{\varphi}_1', ..., \boldsymbol{\varphi}_m')'$ are vectors containing the parameters in $\mathbf{h}_t$ and $\mathbf{g}_t$, respectively. Assume that $\boldsymbol{\varphi} = (\boldsymbol{\psi}', \boldsymbol{\tau}')'$, where

$\boldsymbol{\psi} = (\boldsymbol{\psi}_1', ..., \boldsymbol{\psi}_m')'$ and $\boldsymbol{\tau} = (\boldsymbol{\tau}_1', ..., \boldsymbol{\tau}_m')'$. For each i, $i = 1, ..., m$, denote $\boldsymbol{\phi}_i = (\omega_i, \boldsymbol{\alpha}_{i1}', \ldots, \boldsymbol{\alpha}_{im}', \boldsymbol{\beta}_i')'$, where $\boldsymbol{\alpha}_{ij} = (\alpha_{1ij}, \ldots, \alpha_{q_iij})'$ and $\boldsymbol{\beta}_i = (\beta_{1i}, \ldots, \beta_{p_ii})'$, $\boldsymbol{\varphi}_i = (\omega_i^*, \boldsymbol{\alpha}_{i1}^{*\prime}, \ldots, \boldsymbol{\alpha}_{im}^{*\prime}, \boldsymbol{\beta}_i^{*\prime})$, where $\boldsymbol{\alpha}_{ij}^* = (\alpha_{1ij}^*, \ldots, \alpha_{q_iij}^*)'$, $\boldsymbol{\beta}_i^* = (\beta_{1i}^*, \ldots, \beta_{p_ii}^*)'$, and $\boldsymbol{\tau}_i = (\gamma_i, \mathbf{c}_i)'$ with $\mathbf{c}_i = (c_{i1}, \ldots, c_{ik_i})'$. The identity matrix $\mathbf{I}$ is of size $m \times m$ unless otherwise stated by a subscript. Furthermore, assume the subscript 0 denotes quantities evaluated at the true parameter values and the "hat" denotes the maximum likelihood estimator under the null hypothesis. Thus, the true parameter vector equals $\boldsymbol{\theta}_0 = (\boldsymbol{\vartheta}_0', \boldsymbol{\rho}_0')'$, where $\boldsymbol{\vartheta}_0 = (\boldsymbol{\phi}_0', \boldsymbol{\varphi}_0')'$.

Under the assumption of normality, $\boldsymbol{\varepsilon}_t | \mathcal{F}_{t-1} \sim \mathcal{N}(\mathbf{0}, \boldsymbol{\Sigma}_t)$, the conditional log-likelihood function for observation t is defined as

$$\begin{aligned} \ell_t(\boldsymbol{\theta}) &= -(m/2)\ln(2\pi) - (1/2)\ln|\boldsymbol{\Sigma}_t| - (1/2)\boldsymbol{\varepsilon}_t'\boldsymbol{\Sigma}_t^{-1}\boldsymbol{\varepsilon}_t \\ &= -(m/2)\ln(2\pi) - \ln|\mathbf{D}_t| - (1/2)\ln|\mathbf{P}_t| - (1/2)\mathbf{z}_t'\mathbf{P}_t^{-1}\mathbf{z}_t \end{aligned} \tag{9}$$

and maximising $L_T(\boldsymbol{\theta}) = \sum_{t=1}^T \ell_t(\boldsymbol{\theta})$ with respect to $\boldsymbol{\theta}$ yields the maximum likelihood estimator $\widehat{\boldsymbol{\theta}}$. Equation (9) implies the following decomposition of the log-likelihood function for observation t:

$$\ell_t(\boldsymbol{\phi}, \boldsymbol{\varphi}, \boldsymbol{\rho}) = \ell_t^V(\boldsymbol{\phi}, \boldsymbol{\varphi}) + \ell_t^C(\boldsymbol{\phi}, \boldsymbol{\varphi}, \boldsymbol{\rho}) \tag{10}$$

where the volatility component is

$$\ell_t^V(\boldsymbol{\phi}, \boldsymbol{\varphi}) = \sum_{i=1}^m \ell_{it}^V(\boldsymbol{\phi}_i, \boldsymbol{\varphi}_i) \tag{11}$$

$$= -(1/2)\left\{m\ln(2\pi) + 2\ln|\mathbf{D}_t| + \boldsymbol{\varepsilon}_t'\mathbf{D}_t^{-1}\mathbf{D}_t^{-1}\boldsymbol{\varepsilon}_t\right\} \tag{12}$$

and the correlation term equals

$$\ell_t^C(\boldsymbol{\phi}, \boldsymbol{\varphi}, \boldsymbol{\rho}) = -(1/2)\left\{\ln|\mathbf{P}_t| + \mathbf{z}_t'\mathbf{P}_t^{-1}\mathbf{z}_t - \mathbf{z}_t'\mathbf{z}_t\right\} \tag{13}$$

Using decomposition (10), maximum likelihood estimation of $\boldsymbol{\theta}$ can be carried out in two steps similarly to the two-step approach suggested by Engle (2002) for estimating the DCC-GARCH model. Yet, due to the higher-dimensional parameter space, the estimation of

parameters by full maximum likelihood is time-demanding and numerically challenging. One solution to alleviate the computational burden is to apply the equation-by-equation estimation suggested by Francq and Zakoïan (2016). The assumption of diagonality of $\mathbf{B}_j$ and $\mathbf{B}_j^\star$ enables the estimation of the variance equations separately allowing for cross-market volatility interactions. This formulation facilitates the estimation of the model even when the covariance matrix is of large dimension. The equation-by-equation estimation proceeds in two steps:

1. Estimate $\boldsymbol{\phi}_i$ and $\boldsymbol{\varphi}_i$ equation-by-equation by maximising

$$\begin{aligned} L_{iT}^V(\boldsymbol{\phi}_i, \boldsymbol{\varphi}_i) &= \sum_{t=1}^{T} \ell_{it}^V(\boldsymbol{\phi}_i, \boldsymbol{\varphi}_i) \\ &= -(1/2) \sum_{t=1}^{T} \left\{ \ln(2\pi) + \ln(h_{it}(\boldsymbol{\phi}_i) + g_{it}(\boldsymbol{\varphi}_i)) + \frac{\varepsilon_{it}^2}{h_{it}(\boldsymbol{\phi}_i) + g_{it}(\boldsymbol{\varphi}_i)} \right\} \end{aligned} \tag{14}$$

   with respect to $\boldsymbol{\phi}_i$ and $\boldsymbol{\varphi}_i$ for each i, $i = 1, \ldots, m$, separately. This yields the estimators $\widehat{\boldsymbol{\phi}}_i$ and $\widehat{\boldsymbol{\varphi}}_i$, $i = 1, ..., m$.

2. After estimating the volatility equations, obtain $\widehat{\boldsymbol{\rho}}$ given $\widehat{\boldsymbol{\phi}}_i$ and $\widehat{\boldsymbol{\varphi}}_i$ by maximising

$$L_T^C(\boldsymbol{\rho} | \widehat{\boldsymbol{\phi}}, \widehat{\boldsymbol{\varphi}}) = -(1/2) \sum_{t=1}^{T} \left\{ \ln |\mathbf{P}_t(\boldsymbol{\rho})| + \mathbf{z}_t' \mathbf{P}_t^{-1}(\boldsymbol{\rho}) \mathbf{z}_t - \mathbf{z}_t' \mathbf{z}_t \right\} \tag{15}$$

   where $\mathbf{z}_t = (z_{1t}, ..., z_{mt})'$ with $z_{it} = \varepsilon_{it} / (h_{it}(\widehat{\boldsymbol{\phi}}_i) + g_{it}(\widehat{\boldsymbol{\varphi}}_i))^{1/2}$, $i = 1, ..., m$.

3.2 The score and the Hessian of the log-likelihood function

In order to define the first and second partial derivatives of (9), denote the score vector for observation t as $\mathbf{s}_t(\boldsymbol{\theta}) = \partial \ell_t(\boldsymbol{\theta}) / \partial \boldsymbol{\theta}$ and let

$$\mathbf{s}(\boldsymbol{\theta}) = (1/T) \sum_{t=1}^{T} \mathbf{s}_t(\boldsymbol{\theta}) = (1/T) \sum_{t=1}^{T} \left(\frac{\partial \ell_t(\boldsymbol{\theta})}{\partial \boldsymbol{\vartheta}'}, \frac{\partial \ell_t(\boldsymbol{\theta})}{\partial \boldsymbol{\rho}'} \right)' \tag{16}$$

be the average score. The score vector of (9) has the following form

$$\mathbf{s}_t(\boldsymbol{\theta}) = (\mathbf{s}_t(\boldsymbol{\vartheta})', \mathbf{s}_t(\boldsymbol{\rho})')' \tag{17}$$

where $\mathbf{s}_t(\boldsymbol{\vartheta}) = (\mathbf{s}_t(\boldsymbol{\vartheta}_1)', ..., \mathbf{s}_t(\boldsymbol{\vartheta}_m)')'$ is partitioned into $\mathbf{s}_t(\boldsymbol{\vartheta}_i) = (\mathbf{s}_t(\boldsymbol{\phi}_i)', \mathbf{s}_t(\boldsymbol{\varphi}_i)')'$, $i = 1, ..., m$. The notation $\mathbf{s}_t(\widehat{\boldsymbol{\theta}})$ defines the score evaluated at the maximum likelihood estimator $\widehat{\boldsymbol{\theta}}$.

The analytical expressions of the first partial derivatives of (9) with respect to $\boldsymbol{\theta}$ are given in the following lemma.

Lemma 3.1. *The blocks of the ith element of the score vector (17) for observation t have the following representation*

$$\mathbf{s}_t(\boldsymbol{\vartheta}_i) = \frac{\partial \ell_{it}(\boldsymbol{\theta})}{\partial \boldsymbol{\vartheta}_i} = -(1/2)\frac{1}{\sigma_{it}^2}\frac{\partial \sigma_{it}^2}{\partial \boldsymbol{\vartheta}_i}\left(1 - \mathbf{z}_t'\mathbf{e}_i\mathbf{e}_i'\mathbf{P}_t^{-1}\mathbf{z}_t\right), i = 1, ..., m, \tag{18}$$

$$\mathbf{s}_t(\boldsymbol{\rho}) = \frac{\partial \ell_t(\boldsymbol{\theta})}{\partial \boldsymbol{\rho}} = -(1/2)\frac{\partial \text{vec}(\mathbf{P}_t)'}{\partial \boldsymbol{\rho}}\{\text{vec}(\mathbf{P}_t^{-1}) - \mathbf{P}_t^{-1}\mathbf{z}_t\mathbf{z}_t'\mathbf{P}_t^{-1}\} \tag{19}$$

where the vec(·) operator stacks the columns of the matrix underneath one another, $\mathbf{e}_i = (\mathbf{0}_{i-1}', 1, \mathbf{0}_{m-i}')'$ *and*

$$\frac{\partial \sigma_{it}^2}{\partial \boldsymbol{\vartheta}_i} = \left(\frac{\partial \sigma_{it}^2}{\partial \boldsymbol{\phi}_i'}, \frac{\partial \sigma_{it}^2}{\partial \boldsymbol{\varphi}_i'}, \frac{\partial \sigma_{it}^2}{\partial \boldsymbol{\tau}_i'}\right)' \tag{20}$$

with

$$\frac{\partial \sigma_{it}^2}{\partial \boldsymbol{\vartheta}_i} = \boldsymbol{\omega}_{it} + \sum_{k=1}^{p_i}(\beta_{ik} + \beta_{ik}^* G_i(t/T))\frac{\partial \sigma_{i,t-k}^2}{\partial \boldsymbol{\vartheta}_i} \tag{21}$$

where $\boldsymbol{\omega}_{it} = (\boldsymbol{\upsilon}_{it}', \boldsymbol{\upsilon}_{it}' G_i(t/T), \mathbf{g}_{\tau_{it}}'(g_{it}/G_i(t/T)))'$, *with* $\boldsymbol{\upsilon}_{it} = (1, \boldsymbol{\varepsilon}_{i,t-1}^2, ..., \boldsymbol{\varepsilon}_{i,t-q_i}^2, h_{i,t-1}, ..., h_{i,t-p_i})'$ *and* $\mathbf{g}_{\tau_{it}} = (g_{\gamma_i t}, \mathbf{g}_{c_i t}')'$ *with* $\mathbf{g}_{c_i t} = (g_{c_{i1}t}, \ldots, g_{c_{ik_i}t})'$, $i = 1, \ldots, m$. *The blocks of* $\mathbf{g}_{\tau_{it}}$ *are*

$$g_{\gamma_i t} = \frac{\partial G_i(t/T)}{\partial \gamma_i} = G_i(t/T)(1 - G_i(t/T))\prod_{k=1}^{k_i}(t/T - c_{ik})$$

$$g_{c_{ik}t} = \frac{\partial G_i(t/T)}{\partial c_{ik}} = -\gamma_i G_i(t/T)(1 - G_i(t/T))\prod_{l=1, l\neq k}^{k_i - 1}(t/T - c_{il}), \quad i = 1, \ldots, m.$$

Proof. The expressions for the blocks in (18)-(19) are proven in Appendix 12 of Silvennoinen and Teräsvirta (2017). ∎

The population information matrix equals

$$\mathcal{I}_T(\boldsymbol{\theta}_0) = (1/T)\mathsf{E}\mathbf{s}(\boldsymbol{\theta}_0)\mathbf{s}(\boldsymbol{\theta}_0)' = \mathsf{E}\mathbf{s}_t(\boldsymbol{\theta}_0)\mathbf{s}_t(\boldsymbol{\theta}_0)' \tag{22}$$

where $\mathbf{s}_t(\boldsymbol{\theta}_0)$ is the score evaluated at the true parameter vector $\boldsymbol{\theta}_0$. The negative of the

expected Hessian matrix evaluated at $\boldsymbol{\theta}_0$ equals

$$\mathcal{J}_T(\boldsymbol{\theta}_0) = -(1/T)\mathsf{E}[\mathcal{H}_T(\boldsymbol{\theta}_0)] = -(1/T)\mathsf{E}\sum_{t=1}^{T}\frac{\partial^2\ell_t(\boldsymbol{\theta}_0)}{\partial\boldsymbol{\theta}\partial\boldsymbol{\theta}'}. \tag{23}$$

The Hessian for observation t of the log-likelihood function (9) has the partitioned form

$$\mathcal{H}_t(\boldsymbol{\theta}) = \frac{\partial^2\ell_t(\boldsymbol{\theta})}{\partial\boldsymbol{\theta}\partial\boldsymbol{\theta}'} = \begin{bmatrix} \mathcal{H}_{\boldsymbol{\vartheta}\boldsymbol{\vartheta},t}(\boldsymbol{\theta}) & \mathcal{H}_{\boldsymbol{\vartheta}\boldsymbol{\rho},t}(\boldsymbol{\theta}) \\ \mathcal{H}_{\boldsymbol{\rho}\boldsymbol{\vartheta},t}(\boldsymbol{\theta}) & \mathcal{H}_{\boldsymbol{\rho}\boldsymbol{\rho},t}(\boldsymbol{\theta}) \end{bmatrix} = \begin{bmatrix} \frac{\partial^2\ell_t(\boldsymbol{\theta})}{\partial\boldsymbol{\vartheta}\partial\boldsymbol{\vartheta}'} & \frac{\partial^2\ell_t(\boldsymbol{\theta})}{\partial\boldsymbol{\vartheta}\partial\boldsymbol{\rho}'} \\ \frac{\partial^2\ell_t(\boldsymbol{\theta})}{\partial\boldsymbol{\rho}\partial\boldsymbol{\vartheta}'} & \frac{\partial^2\ell_t(\boldsymbol{\theta})}{\partial\boldsymbol{\rho}\partial\boldsymbol{\rho}'} \end{bmatrix} \tag{24}$$

where the elements for the sub-blocks in (24) are given in the following lemma.

Lemma 3.2. *The sub-blocks of the second-order partial derivatives of the log-likelihood function (14) for observation t are given by*

$$\mathcal{H}_{\boldsymbol{\vartheta}_i\boldsymbol{\vartheta}_j,t}(\boldsymbol{\theta}) = \frac{\partial^2\ell_{it}(\boldsymbol{\theta})}{\partial\boldsymbol{\vartheta}_i\partial\boldsymbol{\vartheta}_j'} = -(1/4)\frac{1}{\sigma_{it}^2\sigma_{jt}^2}\frac{\partial\sigma_{it}^2}{\partial\boldsymbol{\vartheta}_i}\frac{\partial\sigma_{jt}^2}{\partial\boldsymbol{\vartheta}_j'}\left(\mathbf{e}_i'\mathbf{P}_t^{-1}\mathbf{e}_j\mathbf{e}_j'\mathbf{z}_t\mathbf{z}_t'\mathbf{e}_i\right) \tag{25}$$

for $i \neq j$, i,j=1,...,m,

$$\begin{aligned}\mathcal{H}_{\boldsymbol{\vartheta}_i\boldsymbol{\vartheta}_i,t}(\boldsymbol{\theta}) = \frac{\partial^2\ell_{it}(\boldsymbol{\theta})}{\partial\boldsymbol{\vartheta}_i\partial\boldsymbol{\vartheta}_i'} &= -(1/2)\frac{1}{\sigma_{it}^2}\left(\frac{1}{\sigma_{it}^2}\frac{\partial\sigma_{it}^2}{\partial\boldsymbol{\vartheta}_i}\frac{\partial\sigma_{it}^2}{\partial\boldsymbol{\vartheta}_i'} - \frac{\partial^2\sigma_{it}^2}{\partial\boldsymbol{\vartheta}_i\partial\boldsymbol{\vartheta}_i'}\right)\left(\mathbf{e}_i'\mathbf{P}_t^{-1}\mathbf{z}_t\mathbf{z}_t'\mathbf{e}_i - 1\right) \\ &\quad - (1/4)\frac{1}{(\sigma_{it}^2)^2}\frac{\partial\sigma_{it}^2}{\partial\boldsymbol{\vartheta}_i}\frac{\partial\sigma_{it}^2}{\partial\boldsymbol{\vartheta}_i'}\mathbf{e}_i'\mathbf{P}_t^{-1}\left(\mathbf{I} + \mathbf{e}_i\mathbf{e}_i'\right)\mathbf{z}_t\mathbf{z}_t'\mathbf{e}_i\end{aligned} \tag{26}$$

for $i = j$, i=1,...,m,

$$\mathcal{H}_{\boldsymbol{\vartheta}_i\boldsymbol{\rho},t}(\boldsymbol{\theta}) = \frac{\partial^2\ell_{it}(\boldsymbol{\theta})}{\partial\boldsymbol{\vartheta}_i\partial\boldsymbol{\rho}} = -(1/2)\frac{1}{\sigma_{it}^2}\frac{\partial\sigma_{it}^2}{\partial\boldsymbol{\vartheta}_i}(\mathbf{e}_i\otimes\mathbf{e}_i)'(\mathbf{z}_t\mathbf{z}_t'\mathbf{P}_t^{-1}\otimes\mathbf{P}_t^{-1})\frac{\partial\mathrm{vec}(\mathbf{P}_t)}{\partial\boldsymbol{\rho}} \tag{27}$$

and

$$\begin{aligned}\mathcal{H}_{\boldsymbol{\rho}\boldsymbol{\rho},t}(\boldsymbol{\theta}) = \frac{\partial^2\ell_{it}(\boldsymbol{\theta})}{\partial\boldsymbol{\rho}\partial\boldsymbol{\rho}'} &= -(1/2)\frac{\partial\mathrm{vec}(\mathbf{P}_t)}{\partial\boldsymbol{\rho}'}\{\mathbf{P}_t^{-1}\otimes\mathbf{P}_t^{-1} - (\mathbf{P}_t^{-1}\mathbf{z}_t\mathbf{z}_t'\mathbf{P}_t^{-1}\otimes\mathbf{P}_t^{-1} \\ &\quad + \mathbf{P}_t^{-1}\otimes\mathbf{P}_t^{-1}\mathbf{P}_t^{-1}\mathbf{z}_t\mathbf{z}_t'\mathbf{P}_t^{-1})\}\frac{\partial\mathrm{vec}(\mathbf{P}_t)}{\partial\boldsymbol{\rho}}\end{aligned} \tag{28}$$

where $\otimes$ denotes the Kronecker product.

Proof. See Appendix 12 of Silvennoinen and Teräsvirta (2017). The analytical expressions

for each element of $\partial^2\sigma_{it}^2/\partial\boldsymbol{\vartheta}_i\partial\boldsymbol{\vartheta}_i'$ can be obtained by straightforward calculation. ∎

The expressions for $\partial \text{vec}(\mathbf{P}_t)'/\partial\boldsymbol{\rho}$ depend on the form of the correlation structure. For further details we refer to Bollerslev (1990) for constant conditional correlations, Engle (2002) for dynamic conditional correlations and Silvennoinen and Teräsvirta (2015, 2017) when the (un)conditional correlations are assumed to change smoothly over time.

3.3 Asymptotic properties

Under mild regularity conditions, Ling and McAleer (2003) established consistency and asymptotic normality of the QMLE for the general class of vector ARMA-GARCH models (without any diagonality assumption) with constant conditional correlations. Moreover, strict stationarity and ergodicity are also proved for these models. In a restricted formulation, consistency of the QMLE estimator for the ECCC-GARCH model was established by Jeantheau (1998) and the condition for the existence of the fourth-order moment was derived by He and Teräsvirta (2004). Recently, Francq and Zakoïan (2016) showed strong consistency and asymptotic normality of the equation-by-equation estimator of the augmented GARCH model with constant conditional correlations. They show that when the errors differ from the normal distribution, the equation-by-equation estimator is also asymptotically more efficient than the quasi-maximum likelihood approach when the parameters are jointly estimated. The asymptotic results of the second-step of the equation-by-equation estimator need yet to be further investigated.

Since under the null of constant volatility interactions, our model with constant conditional correlations collapses into the augmented GARCH model of Francq and Zakoïan (2016), we can rely on their following result. Under suitable assumptions and regularity conditions, the asymptotic distribution of the equation-by-equation estimator is

$$\sqrt{T}(\widehat{\boldsymbol{\theta}}_T - \boldsymbol{\theta}_0) \xrightarrow{d} \mathcal{N}(\mathbf{0}, \mathcal{J}_T^{-1}(\boldsymbol{\theta}_0)\mathcal{I}_T(\boldsymbol{\theta}_0)\mathcal{J}_T^{-1}(\boldsymbol{\theta}_0)) \tag{29}$$

where $\mathcal{I}_T(\boldsymbol{\theta}_0)$ and $\mathcal{J}_T(\boldsymbol{\theta}_0)$ can be consistently estimated by

$$\mathcal{I}_T(\widehat{\boldsymbol{\theta}}_T) = (1/T)\sum_{t=1}^{T} \mathbf{s}_t(\widehat{\boldsymbol{\theta}}_T)\mathbf{s}_t(\widehat{\boldsymbol{\theta}}_T)' \tag{30}$$

and

$$\mathcal{J}_T(\widehat{\boldsymbol{\theta}}_T) = -(1/T)\sum_{t=1}^{T} \frac{\partial^2 \ell_t(\widehat{\boldsymbol{\theta}}_T)}{\partial \boldsymbol{\theta} \partial \boldsymbol{\theta}'}, \tag{31}$$

respectively. If we further assume $\mathbf{z}_t|\mathcal{F}_{t-1} \sim \mathcal{N}(\mathbf{0}, \mathbf{P})$, then $\mathcal{I}_T(\boldsymbol{\theta}_0) = -\mathsf{E}[\mathcal{J}_T(\boldsymbol{\theta}_0)]$ and the asymptotic covariance matrix reduces to $\mathcal{I}_T^{-1}(\boldsymbol{\theta}_0)$.

Extending their asymptotic results to our model is a nontrivial problem and beyond the scope of the present paper. For inference, we shall assume that the asymptotic distribution of the equation-by-equation estimator is normal. It then follows that

$$\sqrt{T}(\widehat{\boldsymbol{\theta}}_T - \boldsymbol{\theta}_0) \xrightarrow{d} \mathcal{N}(\mathbf{0}, \mathcal{I}_T^{-1}(\boldsymbol{\theta}_0)). \tag{32}$$

4 Testing the adequacy of the extended vector GARCH model

In this section, first we shall introduce a statistical test against a general form of additive misspecification in the extended vector GARCH process and thereafter we focus our attention on the specific form of tests for parameter constancy against smooth changes in the conditional variance equations.

4.1 The general misspecification test

One may expect that over a long observation period, certain economic, environmental and social events affecting the financial institutions cause the structure of volatility to change over time. Similarly, volatility transmissions between markets are very likely to behave differently across tranquil and turbulent times. It thus seems inappropriate to assume that the parameters remain constant when the series of returns to be modelled is long. Testing the constancy of parameters is therefore an important statistical tool to validate the specification of the estimated model. A rejection of the hypothesis of parameter constancy against an additive time-dependent vector GARCH model might be seen as evidence of the hypothesis of time-varying volatility parameters. Of course, other types of misspecification are also possible. Since the rejection of the null hypothesis does not imply that the data have been

generated by the time-varying extended conditional correlation (TV-ECC-) GARCH model, the LM-type test can be viewed as a general misspecification test for multivariate GARCH models.

We shall start with the general misspecification hypothesis for which tests against specific alternatives can be easily derived and then we present explicit formulas for the alternative of interest. In order to shorten the notation, let $h_{it} = h_{it}(\boldsymbol{\phi}_i)$ and $g_{it} = g_{it}(\boldsymbol{\varphi}_i)$, $i = 1, ..., m$, where the additional component g_{it} is an $\mathcal{F}_{t-1}-$measurable function depending on the additional parameters $\boldsymbol{\varphi}_i$. In what follows, assume that the true process of the conditional variance is additively misspecified by introducing a new component

$$\begin{aligned} \varepsilon_{it} &= \sigma_{it} z_{it}, z_{it} \qquad i = 1, ..., m \qquad (33) \\ \sigma_{it}^2 &= h_{it}(\boldsymbol{\phi}_i) + g_{it}(\boldsymbol{\varphi}_i), \qquad (34) \end{aligned}$$

where the errors $z_{it}, i = 1, ..., m$, form a sequence of independent random variables with mean zero and variance one. The function $g_{it} = g_{it}(\boldsymbol{\varphi}_i)$ is at least twice continuously differentiable with respect to $\boldsymbol{\varphi}_i$, such that under the null hypothesis $g_{it}(\boldsymbol{\varphi}_i) = 0$ if and only if $\boldsymbol{\varphi}_i = \mathbf{0}$. Since $\mathbf{D}_t$ is diagonal, it follows that the Gaussian quasi-log-likelihood function (12) is further simplified to

$$\ell_{it}(\boldsymbol{\theta}) = -(1/2)\{\ln 2\pi + \ln\{h_{it}(\boldsymbol{\phi}_i) + g_{it}(\boldsymbol{\varphi}_i)\} + \frac{\varepsilon_{it}^2}{h_{it}(\boldsymbol{\phi}_i) + g_{it}(\boldsymbol{\varphi}_i)}\}. \qquad (35)$$

The average score of (35) is partitioned as

$$\mathbf{s}(\boldsymbol{\vartheta}_i) = (\mathbf{s}_{\boldsymbol{\phi}}(\boldsymbol{\vartheta}_i)', \mathbf{s}_{\boldsymbol{\varphi}}(\boldsymbol{\vartheta}_i)')' \qquad (36)$$

with

$$\mathbf{s}(\boldsymbol{\vartheta}_i) = (1/T)\sum_{t=1}^{T} \frac{\partial \ell_{it}(\boldsymbol{\theta})}{\partial \boldsymbol{\vartheta}_i} = (2T)^{-1}\sum_{t=1}^{T}(z_{it}^2 - 1)\mathbf{x}_{it}, \qquad (37)$$

where $z_{it} = \varepsilon_{it}/(h_{it} + g_{it})^{1/2}$ and $\mathbf{x}_{it} = (\mathbf{x}_{1i,t}', \mathbf{x}_{2i,t}')'$, with $\mathbf{x}_{1i,t} = (h_{it} + g_{it})^{-1}(\partial h_{it}/\partial \boldsymbol{\phi}_i)$ and $\mathbf{x}_{2i,t} = (h_{it} + g_{it})^{-1}(\partial g_{it}/\partial \boldsymbol{\varphi}_i)$.

Setting $\widehat{h}_{it} = h_{it}(\widehat{\boldsymbol{\phi}}_{iT})$, $\widehat{g}_{it} = g_{it}(\widehat{\boldsymbol{\varphi}}_{iT})$ and $\widehat{z}_{it} = \varepsilon_{it}/(\widehat{h}_{it}+\widehat{g}_{it})^{1/2}$, the average score evaluated

at $\widehat{\boldsymbol{\vartheta}}_T$ under the null hypothesis yields

$$\mathbf{s}(\widehat{\boldsymbol{\phi}}_{iT}, \mathbf{0}) = (\mathbf{0}', \mathbf{s}_{\boldsymbol{\varphi}}(\widehat{\boldsymbol{\phi}}_{iT}, \mathbf{0})')' \tag{38}$$

where

$$\mathbf{s}_{\boldsymbol{\varphi}}(\widehat{\boldsymbol{\phi}}_{iT}, \mathbf{0}) = (2T)^{-1} \sum_{t=1}^{T} (\widehat{z}_{it}^2 - 1) \widehat{\mathbf{x}}_{2i,t}|_{H_{0i}} \tag{39}$$

is the relevant (nonzero) block in the LM test statistic. It follows that, under regularity conditions, $\widehat{\boldsymbol{\phi}}_{iT} \longrightarrow \boldsymbol{\phi}_{i0}$ and $\widehat{\boldsymbol{\varphi}}_{iT} \longrightarrow \boldsymbol{\varphi}_{i0}$ in probability as $T \longrightarrow \infty$.

Denoting

$$\mathcal{I}_{iT}(\boldsymbol{\vartheta}_0) = \mathsf{E}\mathbf{s}(\boldsymbol{\phi}_{i0}, \mathbf{0})\mathbf{s}(\boldsymbol{\phi}_{i0}, \mathbf{0})' = \begin{bmatrix} \mathcal{I}_{\boldsymbol{\phi}\boldsymbol{\phi},i}(\boldsymbol{\vartheta}_0) & \mathcal{I}_{\boldsymbol{\phi}\boldsymbol{\varphi},i}(\boldsymbol{\vartheta}_0) \\ \mathcal{I}_{\boldsymbol{\varphi}\boldsymbol{\phi},i}(\boldsymbol{\vartheta}_0) & \mathcal{I}_{\boldsymbol{\varphi}\boldsymbol{\varphi},i}(\boldsymbol{\vartheta}_0) \end{bmatrix} \tag{40}$$

the corresponding south-east block of the inverse of $\mathcal{I}_{iT}(\widehat{\boldsymbol{\vartheta}}_T)$ evaluated under the null equals

$$\left\{\mathcal{I}_{iT}(\widehat{\boldsymbol{\vartheta}}_T)\right\}^{-1}_{[\boldsymbol{\varphi}_i, \boldsymbol{\varphi}_i]} = \left\{\mathcal{I}_{\boldsymbol{\varphi}\boldsymbol{\varphi},i}(\widehat{\boldsymbol{\vartheta}}_T) - \mathcal{I}_{\boldsymbol{\phi}\boldsymbol{\varphi},i}(\widehat{\boldsymbol{\vartheta}}_T)\mathcal{I}^{-1}_{\boldsymbol{\phi}\boldsymbol{\phi},i}(\widehat{\boldsymbol{\vartheta}}_T)\mathcal{I}_{\boldsymbol{\varphi}\boldsymbol{\phi},i}(\widehat{\boldsymbol{\vartheta}}_T)\right\}^{-1}, \tag{41}$$

where $\mathcal{I}_{lk}(\widehat{\boldsymbol{\vartheta}}_T) = (2T)^{-1} \sum_{t=1}^{T} \widehat{\mathbf{x}}_{lt}\widehat{\mathbf{x}}'_{kt}, l, k = 1, 2$ is a consistent plug-in estimator of $\mathcal{I}_{lk}(\boldsymbol{\vartheta}_0)$ (with the subscript i omitted for notational convenience) under the null hypothesis.

Theorem 1 presents the univariate LM-type statistic for the test against a general additive alternative. Specific alternatives for the test can be easily adapted into our framework, where $\widehat{z}_{it}$ and $\widehat{\mathbf{x}}_{li,t}$, $l = 1, 2$, have to be modified accordingly.

Theorem 1 (**Univariate test statistic**). *Consider the model (33)-(34) and assume that the standard regularity conditions hold. Furthermore, assume that under the null hypothesis* H_{0i} : $\boldsymbol{\varphi}_i = \mathbf{0}$, *the function* $g_{it} = g_{it}(\boldsymbol{\varphi}_i) \equiv 0$ *and the appropriate estimates for* $\mathbf{x}_{it} = (\mathbf{x}'_{1i,t}, \mathbf{x}'_{2i,t})'$ *are defined as* $\widehat{\mathbf{x}}_{1i,t} = h_{it}^{-1}(\widehat{\boldsymbol{\phi}}_i)\frac{\partial h_{it}(\widehat{\boldsymbol{\phi}}_i)}{\partial \boldsymbol{\phi}_i}|_{H_{0i}}$, $\widehat{\mathbf{x}}_{2i,t} = h_{it}^{-1}(\widehat{\boldsymbol{\varphi}}_i)\frac{\partial g_{it}(\widehat{\boldsymbol{\varphi}}_i)}{\partial \boldsymbol{\varphi}_i}|_{H_{0i}}$, *and* $\widehat{\zeta}_{it} = \varepsilon_{it}^2/h_{it}(\widehat{\boldsymbol{\phi}}_i) - 1$. *Let* $\widehat{\boldsymbol{\vartheta}}_T$ *be a consistent estimator of* $\boldsymbol{\vartheta}_0$. *Then, under the null hypothesis* $H_{0i} : \boldsymbol{\varphi}_i = \mathbf{0}$, *the LM type statistic for the volatility equation* i

$$\xi_{LMi} = (1/2) \sum_{t=1}^{T} \widehat{\zeta}_{it}\widehat{\mathbf{x}}'_{2i,t} \left\{\mathcal{I}_{iT}(\widehat{\boldsymbol{\vartheta}}_T)\right\}^{-1}_{[\boldsymbol{\varphi}_i, \boldsymbol{\varphi}_i]} \sum_{t=1}^{T} \widehat{\zeta}_{it}\widehat{\mathbf{x}}_{2i,t} \tag{42}$$

is asymptotically χ^2*-distributed with* $\dim(\boldsymbol{\varphi}_i)$ *degrees of freedom.*

In practice, an asymptotically equivalent test to the LM test in Theorem 1 may be carried out in a straightforward way using auxiliary least squares regressions as follows:

1. Estimate $\boldsymbol{\phi}_i$ by maximum likelihood under H_{0i} and compute $\widehat{\zeta}_{it} = \varepsilon_{it}^2/\widehat{h}_{it} - 1$, $\widehat{\mathbf{x}}_{1i,t} = \frac{1}{\widehat{h}_{it}}\frac{\partial \widehat{h}_{it}}{\partial \boldsymbol{\phi}_i}|_{H_{0i}}$ and $\widehat{\mathbf{x}}_{2i,t} = \frac{1}{\widehat{h}_{it}}\frac{\partial \widehat{g}_{it}}{\partial \boldsymbol{\varphi}_i}|_{H_{0i}}$ for $t = 1, \ldots, T$.

2. Regress $\widehat{\zeta}_{it}$ on $\widehat{\mathbf{x}}_{1i,t}$ and $\widehat{\mathbf{x}}_{2i,t}$, $t = 1, \ldots, T$, and obtain the coefficient of determination R_i^2.

3. Under the null hypothesis, the test statistic

$$\xi_{LMi} = T \times R_i^2 \tag{43}$$

has an asymptotic χ^2 distribution with $\dim(\boldsymbol{\varphi}_i)$ degrees of freedom.

Note that the partial derivatives $\partial \hat{h}_{it}/\partial \boldsymbol{\phi}_i|_{H_{0i}}$ and $\partial \hat{g}_{it}/\partial \boldsymbol{\varphi}_i|_{H_{0i}}$ are computed recursively, where it is assumed $\varepsilon_{i0}^2 = h_{i0} = T^{-1}\sum_{t=1}^{T}\varepsilon_{it}^2$, $i = 1, \ldots, m$, as the initial values in the recursion.

To further examine whether the coefficients of the additive component in the augmented version of equation (34) for each $i = 1, ..., m$, are jointly zero, we propose a multivariate version of the LM-type test statistics (42) or (43). The general procedure involves testing the joint hypothesis of no additive misspecification in the system of variance equations, so that a rejection of the null hypothesis is evidence of model misspecification. The extension of the univariate case to the multivariate case is straightforward and the multivariate test statistic is presented in the Corollary 4.1.

Corollary 4.1 (**Multivariate test statistic**). *Consider the model (33)-(34) and assume that the standard regularity conditions hold. Due to the block-diagonality of the information matrix, under the null hypothesis* $H_0 : \boldsymbol{\varphi} = \mathbf{0}$, *the multivariate LM-type statistic defined by*

$$\xi_{LM} = \sum_{i=1}^{m} \xi_{LMi} \tag{44}$$

where ξ_{LMi} *is given by (42) or (43) for each* $i = 1, ..., m$, *has an asymptotic* χ^2 *distribution with* $\dim(\boldsymbol{\varphi})$ *degrees of freedom.*

The robust versions of the univariate and multivariate test statistics to non-normal innovations can be constructed using the procedure by Wooldridge (1990, 1991). The results of Wooldridge enable us to construct test statistics robust to deviations from distributional assumptions. The approach to calculating the robust univariate test statistic proceeds as follows:

1. Estimate $\boldsymbol{\phi}_i$ consistently by maximum likelihood under the null hypothesis and compute $\widehat{\zeta}_{it} = \varepsilon_{it}^2/\widehat{h}_{it} - 1$, $\widehat{\mathbf{x}}_{1i,t} = \dfrac{1}{\widehat{h}_{it}}\dfrac{\partial \widehat{h}_{it}}{\partial \boldsymbol{\phi}_i}|_{H_{0i}}$ and $\hat{\mathbf{x}}_{2i,t} = \dfrac{1}{\widehat{h}_{it}}\dfrac{\partial \widehat{g}_{it}}{\partial \boldsymbol{\varphi}_i}|_{H_{0i}}$ for $t = 1, \ldots, T$.

2. Regress $\widehat{\mathbf{x}}_{2i,t}$ on $\widehat{\mathbf{x}}_{1i,t}$, $t = 1, ..., T$, and save the vector of residuals $\widehat{\mathbf{r}}_{it}$ from the regression.

3. Regress $\mathbf{1}_T$ on $\widehat{\zeta}_{it}\widehat{\mathbf{r}}_{it}$, $t = 1, ..., T$, and compute the residual sum of squares RSS_i. Under H_{0i}, the robust statistic

$$\xi_{robi} = T - RSS_i \tag{45}$$

has an asymptotic χ^2 distribution with $\dim(\boldsymbol{\varphi}_i)$ degrees of freedom.

For the robust multivariate statistic, repeat the previous steps 1−3, for all $i = 1, ..., m$, and compute the LM-type test statistic

$$\xi_{rob} = \sum_{i=1}^{m} \xi_{robi} \tag{46}$$

which is asymptotically χ^2-distributed with $\dim(\boldsymbol{\varphi})$ degrees of freedom.

4.2 Testing for smoothly time-varying volatility and spillovers

We now consider specific alternatives belonging to the general misspecification test presented in Section 4.1. We begin by deriving the test for parameter constancy against the alternative of a smoothly time-varying augmented GARCH model and next we focus on the volatility-based statistical test of co-movements within this class of models.

In order to derive the misspecification test statistic rewrite the variance equation (34) as:

$$\sigma_{it}^2 = \omega_i + \sum_{j=1}^{m} \alpha_{ij}\varepsilon_{j,t-1}^2 + \beta_i\sigma_{i,t-1}^2 + \left(\omega_i^* + \sum_{j=1}^{m} \alpha_{ij}^*\varepsilon_{j,t-1}^2 + \beta_i^*\sigma_{i,t-1}^2\right)\widetilde{G}_{it}(t/T; \gamma_i, \mathbf{c}_i) \tag{47}$$

where, for simplicity, we restrict our discussion to the case when the augmented GARCH

component is of order one ($p_i = q_i = 1$) in (6)-(7) since first-order models describe well the majority of financial applications. For notational convenience, we let $\widetilde{G}_{it}(t/T;\gamma_i,\mathbf{c}_i) = G_{it}(t/T;\gamma_i,\mathbf{c}_i) - 1/2$ without losing generality.

The null hypothesis of parameter constancy against smoothly time-varying volatility corresponds to testing $H_{0i} : \gamma_i = 0$ against $H_{1i} : \gamma_i > 0$ in (47). When $\gamma_i = 0$ holds, the parameters ω_i^*, α_{ij}^*, β_i^* and $\mathbf{c}_i$, $j = 1,\ldots,m$, constitute a vector of unidentified nuisance parameters. We circumvent the identification problem by approximating $\widetilde{G}_{it}(t/T;\gamma_i,\mathbf{c}_i)$ with its first-order Taylor expansion evaluated at $\gamma_i = 0$ as in Luukkonen et al. (1988). Using Taylor's theorem, we obtain

$$\widetilde{G}_{it}(t/T;\gamma_i,\mathbf{c}_i) = \sum_{k=0}^{k_i} \gamma_i (t/T)^k \tilde{c}_{ik} + R_{it}(t/T;\gamma_i,\mathbf{c}_i) \tag{48}$$

where $R_{it}(t/T;\gamma_i,\mathbf{c}_i)$ is the remainder term. Replacing $\widetilde{G}_{it}(t/T;\gamma_i,\mathbf{c}_i)$ in (47) by (48) and rearranging terms, gives

$$\sigma_{it}^2 = \kappa_i + \sum_{j=1}^{m} a_{ij}\varepsilon_{j,t-1}^2 + b_i\sigma_{i,t-1}^2 + \sum_{k=1}^{k_i}(t/T)^k \left(\kappa_{ik}^* + \sum_{j=1}^{m} a_{ijk}^*\varepsilon_{j,t-1}^2 + b_{ik}^*\sigma_{i,t-1}^2\right) + R_{it}(t/T;\gamma_i,\mathbf{c}_i) \tag{49}$$

where the parameters are functions of the original ones in (47). Under H_{0i}, the remainder $R_{it}(t/T;\gamma_i,\mathbf{c}_i) = 0$, so that the remainder does not affect the asymptotic null distribution of the test statistic. Using (49) we can transform the original testing problem into testing against the following approximate alternative:

$$\varepsilon_{it} = (h_{it} + g_{it})^{1/2} z_{it} \tag{50}$$

where

$$h_{it} + g_{it} = \kappa_i + \sum_{j=1}^{m} a_{ij}\varepsilon_{j,t-1}^2 + b_i(h_{i,t-1} + g_{i,t-1}) \tag{51}$$

$$+ \sum_{k=1}^{k_i} \kappa_{ik}^*(t/T)^k + \sum_{j=1}^{m}\sum_{k=1}^{k_i} a_{ijk}^*(t/T)^k\varepsilon_{j,t-1}^2 + \sum_{j=1}^{m}\sum_{k=1}^{k_i} b_{ik}^*(t/T)^k h_{i,t-1} \tag{52}$$

and

$$g_{it} = b_i g_{i,t-1} + \sum_{k=1}^{k_i} \kappa_{ik}^* (t/T)^k + \sum_{j=1}^{m} \sum_{k=1}^{k_i} a_{ijk}^* (t/T)^k \varepsilon_{j,t-1}^2 + \sum_{j=1}^{m} \sum_{k=1}^{k_i} b_{ik}^* (t/T)^k h_{i,t-1} \tag{53}$$

.

Model (50)-(53) reduces to the null model under the auxiliary null hypothesis of parameter constancy:

$$H_{0i} : \kappa_{ik}^* = a_{ijk}^* = b_{ik}^* = 0, \quad j = 1, \ldots, m, \quad k = 1, ..., k_i. \tag{54}$$

The following corollary defines the test statistic for testing the null hypothesis in (54).

Corollary 4.2. *Consider the model (50)-(53) and let* $\boldsymbol{\phi}_i = (\kappa_i, \mathbf{a}_i', b_i)'$ *with* $\mathbf{a}_i = (a_{i1}, ..., a_{im})'$ *and* $\boldsymbol{\varphi}_i = (\boldsymbol{\kappa}_i^{*\prime}, \mathbf{a}_{i1}^{*\prime}, ..., \mathbf{a}_{im}^{*\prime}, \mathbf{b}_i^{*\prime})'$ *with* $\boldsymbol{\kappa}_i = (\kappa_{i1}, ..., \kappa_{ik_i})'$, $\mathbf{a}_{ij}^* = (a_{ij1}^*, ..., a_{ijk_i}^*)'$ *and* $\mathbf{b}_i = (b_{i1}, ..., b_{ik_i})'$, $i, j = 1, ..., m$, $k = 1, ..., k_i$. *In addition, denote* $\boldsymbol{\upsilon}_{it} = (1, \boldsymbol{\varepsilon}_{t-1}^{2\prime}, h_{i,t-1})'$, $\boldsymbol{\varepsilon}_t = (\varepsilon_{1t}, ..., \varepsilon_{mt})'$, $\mathbf{Z}_{1i,t} = [(t/T)^k \varepsilon_{j,t-1}^2]$ *and* $\mathbf{Z}_{2i,t} = [(t/T)^k h_{i,t-1}]$, $k = 1, ..., k_i$, $i, j = 1, ..., m$. *Under* $H_0 : \boldsymbol{\varphi}_i = \mathbf{0}$, *the LM-type statistic (42) or (43), where*

$$\widehat{\mathbf{x}}_{i1,t} = \frac{1}{\widehat{h}_{it}} \frac{\partial \widehat{h}_{it}}{\partial \boldsymbol{\phi}_i}|_{H_{0i}} = \widehat{h}_{it}^{-1} (\widehat{\boldsymbol{\upsilon}}_{it} + b_i \frac{\partial \widehat{h}_{i,t-1}}{\partial \boldsymbol{\phi}_i}|_{H_{0i}}) \tag{55}$$

$$\widehat{\mathbf{x}}_{i2,t} = \frac{1}{\widehat{h}_{it}} \frac{\partial \widehat{g}_{it}}{\partial \boldsymbol{\varphi}_i}|_{H_{0i}} = \widehat{h}_{it}^{-1} \left(((t/T), ..., (t/T)^{k_i}, vec(\mathbf{Z}_{1i,t})', vec(\mathbf{Z}_{2i,t})')' + b_i \frac{\partial \widehat{g}_{i,t-1}}{\partial \boldsymbol{\varphi}_i}|_{H_{0i}} \right) \tag{56}$$

is asymptotically χ^2*-distributed with* $\dim(\boldsymbol{\varphi}_i)$ *degrees of freedom.*

4.3 Specification of additive extended GARCH models

We design a model-building cycle for the TV-ECC-GARCH model identical to the specific-to-general strategy for nonlinear models recommended by Granger (1993) and Teräsvirta (1998b), among others. The technique involves a sequential procedure for specifying the parameterization of the volatility component and determining the shape of the transition function using a sequence of LM-type tests. Formal asymptotic theory for these tests is not yet available, and thereafter we assume the test statistics to approximate the chi-squared distribution. The modelling cycle for specifying additive extended GARCH models consists of the following stages:

1. Estimate the extended GARCH model as in Francq and Zakoïan (2016). The determination of the lag structure may be done using a model selection criterion. This may be preceded by testing the null hypothesis of no volatility interactions as in Nakatani and Teräsvirta (2009) and Pedersen (2017).

2. Test parameter constancy against the additive time-dependent vector GARCH model (TV-ECC-GARCH) alternative using the LM-type statistic described in Section (4.2) at the significance level $\alpha^{(1)}$: $H_{0i}^{\text{TV-ECC}} : \kappa_{ik}^* = a_{ijk}^* = b_{ik}^* = 0, \quad j = 1, \ldots, m, \quad k = 1, ..., k_i.$ in (54). If $H_{0i}^{\text{TV-ECC}}$ is rejected, then select the order $k \leq 3$ in the exponent of $G_{it}(t/T; \gamma_i, \mathbf{c}_i)$ based on a sequence of nested tests as in Teräsvirta (1994). This is done by testing the following sequence of nested hypotheses:

$$
\begin{aligned}
H_{03i} &: \boldsymbol{\varphi}_{i3} = \mathbf{0} \\
H_{02i} &: \boldsymbol{\varphi}_{i2} = \mathbf{0} \quad | \quad \boldsymbol{\varphi}_{i3} = \mathbf{0} \\
H_{01i} &: \boldsymbol{\varphi}_{i1} = \mathbf{0} \quad | \quad \boldsymbol{\varphi}_{i2} = \boldsymbol{\varphi}_{i3} = \mathbf{0}
\end{aligned}
$$

where $\boldsymbol{\varphi}_{ik} = (\kappa_{ik}^*, a_{i1k}^*, \ldots, a_{imk}^*, b_{ik}^*)'$, $i = 1, \ldots, m, k = 1, 2, 3$, by means of LM-type tests using auxiliary regressions. The choice of k proceeds as follows. Carry out the three sequential tests and observe the hypotheses rejected. If H_{01i} and H_{03i} are rejected more strongly, measured by p-values, than H_{02i}, then select either $k = 1$ or $k = 3$. If testing H_{02i} yields the strongest rejection, then select $k = 2$.

3. If parameter constancy is rejected, then sub-hypotheses are tested to determine whether the TV-ECC-GARCH model is necessary to characterize the data or either whether a model with a subset of time-varying parameters is sufficient. The statistical tests are conducted using the significance level $\alpha^{(2)} = \tau\alpha^{(1)}$, where $\tau \in (0, 1)$. Here we set $\tau = 0.5$. In what follows, assume the partitioned vector $\boldsymbol{\varphi}_{ik} = (\boldsymbol{\varphi}_{ik,1}', \boldsymbol{\varphi}_{ik,2}')'$, where $\boldsymbol{\varphi}_{ik,1} = (\kappa_{ik}^*, a_{ik}^*, b_{ik}^*)'$ denotes the vector of standard GARCH parameters and $\boldsymbol{\varphi}_{ik,2} = \{a_{ijk}^*\}$, $i \neq j, j = 1, \ldots, m$, $k = 1, 2, 3$, denotes the cross-market ARCH coefficients. In order to identify individual changes in the dynamics of volatility (or co-volatility) for a subset of return series, we shall proceed as follows:

(a) Test the hypothesis of parameter constancy in the standard GARCH coefficients

$$H_{0i,1}^{\text{TV-VOL}} : \boldsymbol{\varphi}_{i1,1} = \boldsymbol{\varphi}_{i2,1} = \boldsymbol{\varphi}_{i3,1} = \mathbf{0}_3 \quad | \quad \boldsymbol{\varphi}_{i1,2} = \boldsymbol{\varphi}_{i2,2} = \boldsymbol{\varphi}_{i3,2} = \mathbf{0}.$$

(b) Test the hypothesis of parameter constancy in the cross-market ARCH coefficients

$$H_{0i,2}^{\text{TV-CO-VOL}} : \boldsymbol{\varphi}_{i1,2} = \boldsymbol{\varphi}_{i2,2} = \boldsymbol{\varphi}_{i3,2} = \mathbf{0} \quad | \quad \boldsymbol{\varphi}_{i1,1} = \boldsymbol{\varphi}_{i2,1} = \boldsymbol{\varphi}_{i3,1} = \mathbf{0}.$$

(c) If either $H_{0i,1}^{\text{TV-VOL}}$ or $H_{0i,2}^{\text{TV-CO-VOL}}$ is rejected, then select $k = 1, 2, 3$, by testing the following sequence of nested hypotheses at the significance level $\alpha^{(3)} = \tau\alpha^{(2)}$:

$$\begin{aligned}
H_{03i,s} &: \boldsymbol{\varphi}_{i3,s} = \mathbf{0} \quad | \quad \boldsymbol{\varphi}_{ik,r} = \mathbf{0} \\
H_{02i,s} &: \boldsymbol{\varphi}_{i2,s} = \mathbf{0} \quad | \quad \boldsymbol{\varphi}_{ik,r} = \mathbf{0} \text{ and } \boldsymbol{\varphi}_{i3,s} = \mathbf{0} \\
H_{01i,s} &: \boldsymbol{\varphi}_{i1,s} = \mathbf{0} \quad | \quad \boldsymbol{\varphi}_{ik,r} = \mathbf{0} \text{ and } \boldsymbol{\varphi}_{i3,s} = \boldsymbol{\varphi}_{i2,s} = \mathbf{0},
\end{aligned}$$

for $r \neq s$, $r, s = 1, 2$, by means of auxiliary regressions as before. Rejection of $H_{0i,2}$ provides evidence for time-varying cross-market ARCH effects revealing changes in volatility spillovers between the returns.

An appealing feature of this testing approach is that it makes it possible to identify individual changes in the volatility dynamics (or co-volatility) for a subset of return series. As a result, statistical evidence of time-varying volatility parameters is a necessary, yet not a sufficient condition for volatility-based spillovers. In this framework, rejecting the null hypothesis suggests that the volatility parameters are jointly time-varying, but it does not imply that every coefficient is changing over time. As a matter of fact, the hypothesis for parameter constancy can be rejected when structural changes occur in the volatility dynamics but the co-volatility parameters remain constant.

5 Small sample properties

5.1 Design of the experiments

In this section, we investigate by Monte Carlo simulations the finite sample behaviour of the tests presented in section 4. We shall first report the empirical size and the power results of the parameter constancy tests. Thereafter, we carry out several robustness checks regarding the implementation of the tests. The experiments are conducted for the bivariate, trivariate and five-variate cases, that is, for $m = 2, 3, 5$. We generated 5000 replications at sample sizes $T = 1000, 2500$ and 5000 for each data generating process (DGP). The first 1000 generated observations from each data set have been discarded to reduce initialization effects. For the size simulations we use the bivariate extended conditional constant correlation GARCH model of Jeantheau (1998) whose volatility component is given by

$$\mathbf{h}_t = \boldsymbol{\omega} + \mathbf{A}_1 \boldsymbol{\varepsilon}_{t-1}^2 + \mathbf{B}_1 \mathbf{h}_{t-1} \tag{57}$$

where we restrict the matrix of GARCH parameters $\mathbf{B}_1$ to be diagonal and we let the conditional correlation parameter ρ_{12} to vary between 0.3 and 0.9. The generated data satisfy the weak stationarity condition established in Jeantheau (1998) where the spectral radius of $\mathbf{A} + \mathbf{B}$, denoted by $\lambda(\mathbf{A} + \mathbf{B})$, is smaller than unity. For the power simulations we use the extended version of (57) with time-varying parameter matrices where the model is specified as

$$\mathbf{h}_t = \boldsymbol{\omega} + \mathbf{A}_1 \boldsymbol{\varepsilon}_{t-1}^2 + \mathbf{B}_1 \mathbf{h}_{t-1} + \left(\boldsymbol{\omega}^* + \mathbf{A}_1^* \boldsymbol{\varepsilon}_{t-1}^2 + \mathbf{B}_1^* \mathbf{h}_{t-1}\right) \mathbf{G}_t \tag{58}$$

where $\mathbf{A}$ and $\mathbf{A}^*$ are non-diagonal matrices of ARCH coefficients, $\mathbf{B}$ and $\mathbf{B}^*$ are diagonal matrices of GARCH coefficients and $\mathbf{G}_t$ is the diagonal matrix of logistic transition functions defined in (8). Only parameter combinations satisfying the sufficient conditions for weak stationary in each extreme volatility state are considered. Under these restrictions, the DGPs verify the conditions $\lambda(\mathbf{A} + \mathbf{B}) < 1$ when $\mathbf{G}_t = \mathbf{0}$ and $\lambda(\mathbf{A} + \mathbf{A}^* + \mathbf{B} + \mathbf{B}^*) < 1$ when $\mathbf{G}_t = \mathbf{I}$. All computations have been carried out using the open-source statistical software package R (R Core Team (2017)).

Table 1: Data generating processes for size simulations for tests of parameter constancy

	DGP 1	DGP 2	DGP 3	DGP 4
$\mathbf{A}_1$	$\begin{bmatrix} 0.10 & 0.005 \\ 0.005 & 0.05 \end{bmatrix}$	$\begin{bmatrix} 0.10 & 0.005 \\ 0.005 & 0.05 \end{bmatrix}$	$\begin{bmatrix} 0.10 & 0.07 \\ 0.02 & 0.05 \end{bmatrix}$	$\begin{bmatrix} 0.10 & 0.005 \\ 0.005 & 0.05 \end{bmatrix}$
$\mathbf{B}_1$	$\begin{bmatrix} 0.80 & 0 \\ 0 & 0.85 \end{bmatrix}$	$\begin{bmatrix} 0.80 & 0 \\ 0 & 0.85 \end{bmatrix}$	$\begin{bmatrix} 0.80 & 0 \\ 0 & 0.85 \end{bmatrix}$	$\begin{bmatrix} 0.88 & 0 \\ 0 & 0.94 \end{bmatrix}$
ρ_{12}	0.90	0.30	0.90	0.30
$\lambda(\mathbf{A}_1 + \mathbf{B}_1)$	0.905	0.905	0.937	0.992

Note: The vector of constants in the conditional variances equals $\boldsymbol{\omega} = [0.10 \quad 0.20]'$ for all DGPs.

5.2 Size simulations

To illustrate the behaviour of the parameter constancy test in small samples we present the results from the size simulations. The data generated processes (DGPs) from four bivariate ECC-GARCH(1,1) models used in the size simulations are reported in Table 1. The artificial series have the following dynamics. The persistence in volatility varies from moderate (0.905) in DGP 1-2 to very high (0.992) in DGP 4. DGPs 2 and 4 have low correlations (ρ_{12}=0.3) with moderate and very high persistence, respectively, while DGP 3 is characterised by higher cross-market volatility interactions and high correlations (ρ_{12}=0.9). The simulation study shows that the non-robust tests are severely-size distorted and the robust statistics clearly outperform their non-robust versions. These simulations are available upon request. For the sake of saving space, we only report the actual rejection frequencies for the robust tests statistics when $T = 2500, 5000$.

Size discrepancy plots for the robust tests statistics are displayed in Figure 1. The figures show the size discrepancies, that is, the differences between the actual rejection frequencies and the nominal sizes (vertical axis) plotted against the nominal sizes (horizontal axis). As expected, the size distortions decrease with the number of observations but increase with the level of persistence in volatility. Furthermore, size distortions tend to increase with the level of correlation and decrease with the magnitude of the volatility interactions. Overall, the robust tests have reasonably good size in finite samples with the exception of DGP1 characterised with high correlation and small volatility interactions where size is largely

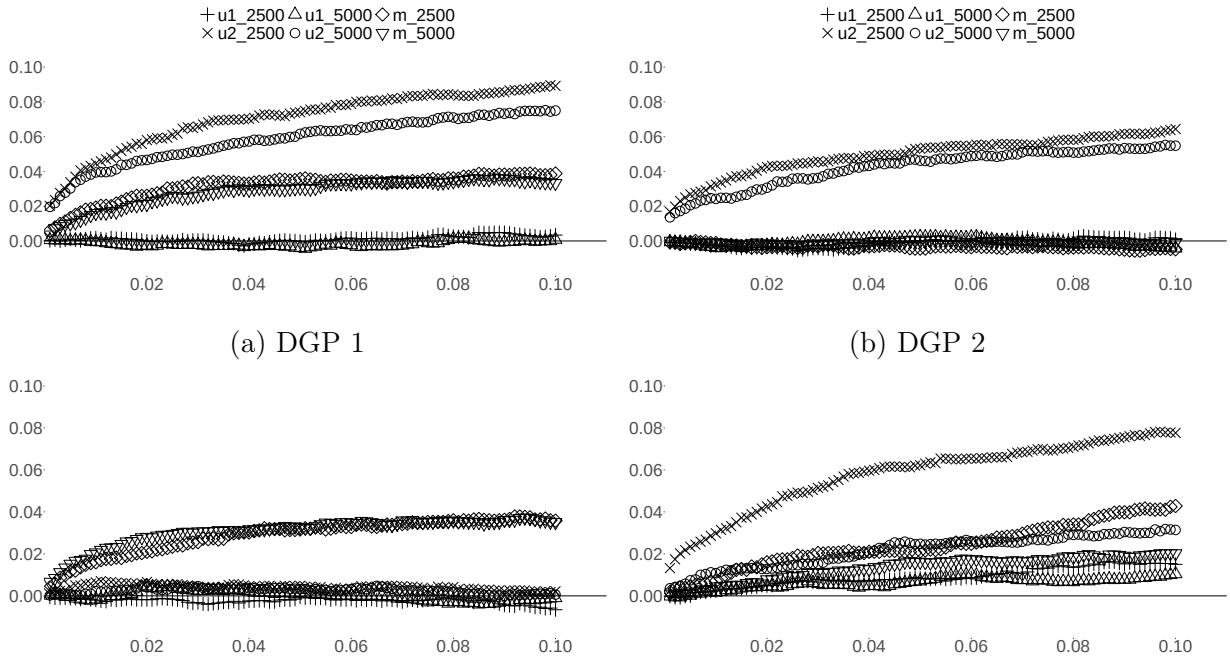

(a) DGP 1

(b) DGP 2

(c) DGP 3

(d) DGP 4

Figure 1: Size discrepancy plots for tests of parameter constancy tests using artificial series generated according to the DGPs in Table 1. The size discrepancy is plotted against the nominal size. Results are shown for the univariate robust (ui_T), $i = 1, 2$, and multivariate robust (m_T) test statistics defined in (45) and (46), respectively, with $\widehat{\mathbf{x}}_{i1,t}$ and $\widehat{\mathbf{x}}_{i2,t}$ given in (56) and (56) for $T = 2500, 5000$. The number of replications for each simulation equals 5000.

distorted. Thus, the test may tend to reject more often when the correlations are large and interactions are small. Looking at the results of the multivariate test, the empirical size is also distorted to some extent. The size properties of the tests suggest that the asymptotic distribution of the test statistics may be a poor approximation of their true distribution in some situations. In order to improve inference and obtain well-behaved tests, bootstrap procedures may be used in order to mitigate the poor size properties in those cases.

5.3 Power simulations

In this section we present the results from the power simulations for the robust test statistics. There is no direct benchmark at which we can compare our tests, but it may be interesting to investigate their power in small samples. We simulate the bivariate model under the alternative using four alternative specifications. The DGPs from (58) are listed in Table 2. The upper panel defines the volatility structure in the first extreme state which is common

Table 2: Data generating processes for power simulations for tests of parameter constancy

$$\boldsymbol{\omega} = \begin{bmatrix} 0.10 & 0.20 \end{bmatrix}' \mathbf{A}_1 = \begin{bmatrix} 0.10 & 0.05 \\ 0.05 & 0.05 \end{bmatrix} \mathbf{B}_1 = \begin{bmatrix} 0.80 & 0 \\ 0 & 0.85 \end{bmatrix}$$

	DGP 5	DGP 6	DGP 7	DGP 8
$\boldsymbol{\omega}^*$			$\begin{bmatrix} 0.20 & 0.10 \end{bmatrix}'$	$\begin{bmatrix} 0.20 & 0.10 \end{bmatrix}'$
$\mathbf{A}_1^*$	$\begin{bmatrix} 0.01 & 0.015 \\ 0.015 & 0.01 \end{bmatrix}$		$\begin{bmatrix} 0.01 & 0.015 \\ 0.015 & 0.01 \end{bmatrix}$	
$\mathbf{B}_1^*$		$\begin{bmatrix} 0.04 & 0 \\ 0 & 0.03 \end{bmatrix}$		$\begin{bmatrix} 0.02 & 0 \\ 0 & 0.03 \end{bmatrix}$
$\lambda\left(\mathbf{A}_1^{(*)} + \mathbf{B}_1^{(*)}\right)$	0.995	0.975	0.995	0.975

Note: In the power simulations, we set $c_{11} = 0.50$, $c_{21} = 0.75$, $\gamma_1 = 5$, $\gamma_2 = 10$ and $\rho = 0.70$ for all DGPs.

to all DGPs and from where parameters change to the second extreme volatility state. The sign and magnitude of the parameters that are changing over time are shown in the lower panel. In DGPs 5 and 6 the ARCH and GARCH parameter matrices are time-varying, respectively. DGPs 7 and 8 have a similar design but the vector of constants is also assumed to be time-dependent. Selected results from the power simulations are displayed in Figure 2. The rejection frequencies for the tests under the generated data behave as expected. The actual rejection frequencies show that power increases notably with the sample size, meaning that a long time series is required for a well-behaved test in terms of power. Detecting time dependence in the volatility interactions can be quite difficult against DGP 5, but the power increases sharply if the true alternative contains additional changes in the constants at all sample sizes. Interestingly, the tests also become less powerful against DGPs when the level of the unconditional correlations is quite large. In general, the power against DGPs clearly increases with the number of time-varying parameters. Therefore, one expects the power of the multivariate test to be clearly stronger compared to that of the univariate parameter constancy test.

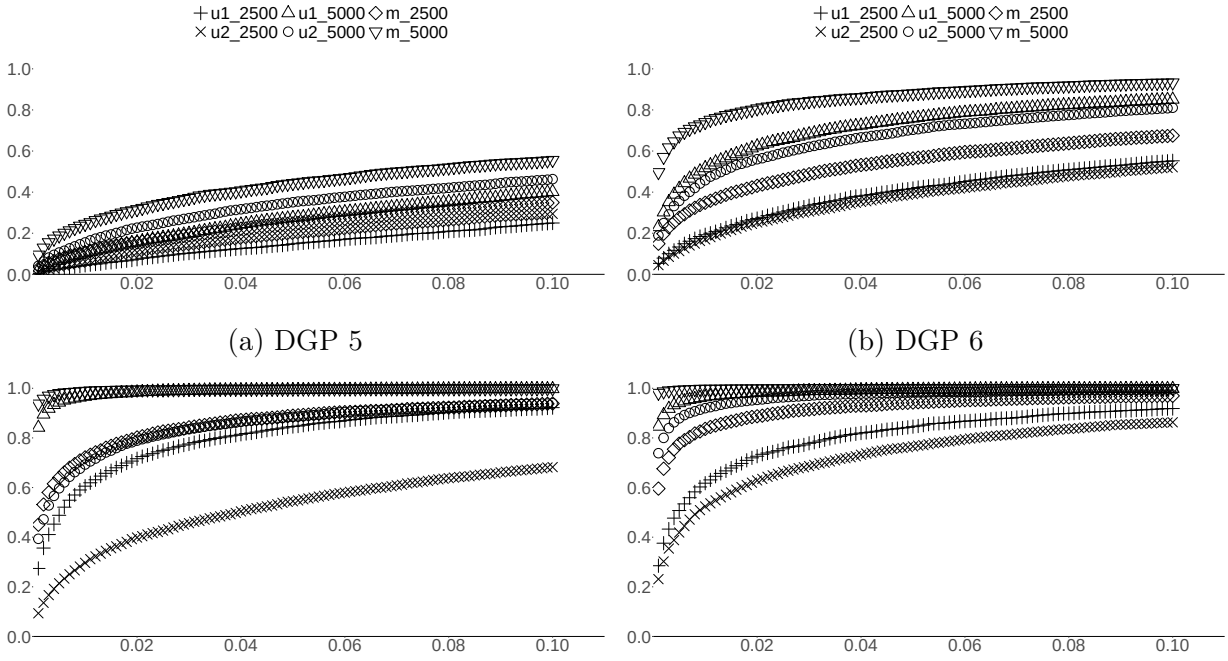

(a) DGP 5

(b) DGP 6

(c) DGP 7

(d) DGP 8

Figure 2: Power curves of the tests for parameter constancy tests using artificial series generated according to the DGPs in Table 2. Results are shown for the univariate robust (ui_T), $i = 1, 2$, and multivariate robust (m_T) test statistics defined in (45) and (46), respectively, with $\widehat{\mathbf{x}}_{i1,t}$ and $\widehat{\mathbf{x}}_{i2,t}$ given in (56) and (56) for $T = 2500, 5000$. The number of replications for each simulation equals 5000.

5.4 Robustness checks

In this section we perform several robustness checks for the parameter constancy tests to investigate how the suggested statistical tests are affected in higher-dimensional models assuming constant conditional correlations. Finite-sample properties of the test statistics are also studied in higher-dimensional models under changing conditional correlations. For the sake of saving space, we omit some information regarding the model parameters used in these simulations and the experiment results of the modelling cycle, but they are available upon request.

Firstly, we shall evaluate the empirical rejection frequencies of the null hypothesis when it is true for given higher-dimensional models described below. For the size simulations, we generated additional artificial DGPs with constant conditional correlations where volatility is moderately persistent with $\lambda(\mathbf{A}_1 + \mathbf{B}_1) = 0.956$ in the 3-dimensional model and $\lambda(\mathbf{A}_1 + \mathbf{B}_1) = 0.971$ in the 5-dimensional model. The size discrepancy plots for the higher dimensional models are depicted in the upper panel of Figure 3. As for higher-dimensional models, both the non-robust and robust multivariate LM test are size-distorted and the empirical size of the tests increases with the dimension of the model, but it decreases with the sample size. Interestingly, the empirical size of the univariate robust LM test remains very close to the nominal size at higher-dimensional models. In summary, the robust version of the multivariate test has notably larger size distortions than those of the univariate test statistic for higher dimensional models.

Secondly, the finite sample size behaviour of the test statistics are also studied for multidimensional models under changing conditional correlations. The statistical tests are derived for cases in which the parametric structure of the GARCH equations may be misspecified with constant conditional correlations. However, it appears to be useful to examine the behaviour of the tests assuming alternative parameterizations for the correlation structure. The alternative bivariate designs used in the simulations are summarised in Table 3. We assume the parameters of the volatility equations to be identical in both designs where volatility has moderate persistence. This is shown in the middle panel of Table 3. The performance for the empirical levels of the test statistics shall be investigated when the true model generating the data is the extended time-varying correlations (ETVC-)GARCH model

Table 3: Data generating processes for size and power simulations under time-varying correlations. In the power simulations, we set $c_{1i} = 0.50$ and $\gamma_i = 5$, $i = 1, 2$ for all DGPs.

$$\mathbf{P}_1 \begin{bmatrix} 1 & 0.25 \\ 0.25 & 1 \end{bmatrix} \quad \mathbf{P}_2 \begin{bmatrix} 1 & 0.75 \\ 0.75 & 1 \end{bmatrix} \quad \bar{\mathbf{Q}} \begin{bmatrix} 1 & 0.50 \\ 0.50 & 1 \end{bmatrix}$$

$$c_1 = 0.50 \quad \gamma = 5 \quad \alpha = 0.05 \ \beta = 0.90$$

ETVC-GARCH(1, 1) MODEL

EDCC-GARCH(1, 1) MODEL

$$\boldsymbol{\omega} \begin{bmatrix} 0.01 & 0.01 \end{bmatrix}' \quad \mathbf{A}_1 \begin{bmatrix} 0.09 & 0.001 \\ 0.004 & 0.04 \end{bmatrix} \quad \mathbf{B}_1 \begin{bmatrix} 0.90 & 0 \\ 0 & 0.89 \end{bmatrix}$$

TV-ETVC-GARCH(1, 1) MODEL

TV-EDCC-GARCH(1, 1) MODEL

$$\boldsymbol{\omega}^* \begin{bmatrix} 0.02 & 0.02 \end{bmatrix}' \quad \mathbf{A}_1^* \begin{bmatrix} 0 & 0.001 \\ 0.01 & 0.01 \end{bmatrix} \quad \mathbf{B}_1^* \begin{bmatrix} 0 & 0 \\ 0 & 0 \end{bmatrix}$$

where the transition variable is the rescaled time. We further examine the empirical size of the LM robust statistics under the extended dynamic conditional correlations (EDCC-) GARCH parameterization. The correlation parameters for both alternatives are specified in the upper panel of Table 3. Size simulation results from both designs are plotted in the lower panel of Figure 3. While the LM robust test statistics is strongly oversized for the constant correlations design, the tests become rather well-behaved assuming time-varying unconditional correlations at all sample sizes. The results (not shown here to conserve space) are also robust to other transition variables such as when a GARCH process is governing the changes in the correlations dynamics. Similar behaviour is observed for the dynamic correlation structure where the empirical size of the tests remains very close to the nominal size. Moreover, the empirical levels of the tests behave similarly for higher correlation persistence. As for the power experiments, a large number of observations is required for the LM robust tests to have reasonable power under time-varying correlation dynamics. Overall, the chi-squared distribution provides a good approximation to the univariate and the multivariate robust test statistics for designs when the (un)conditional correlations are time-varying.

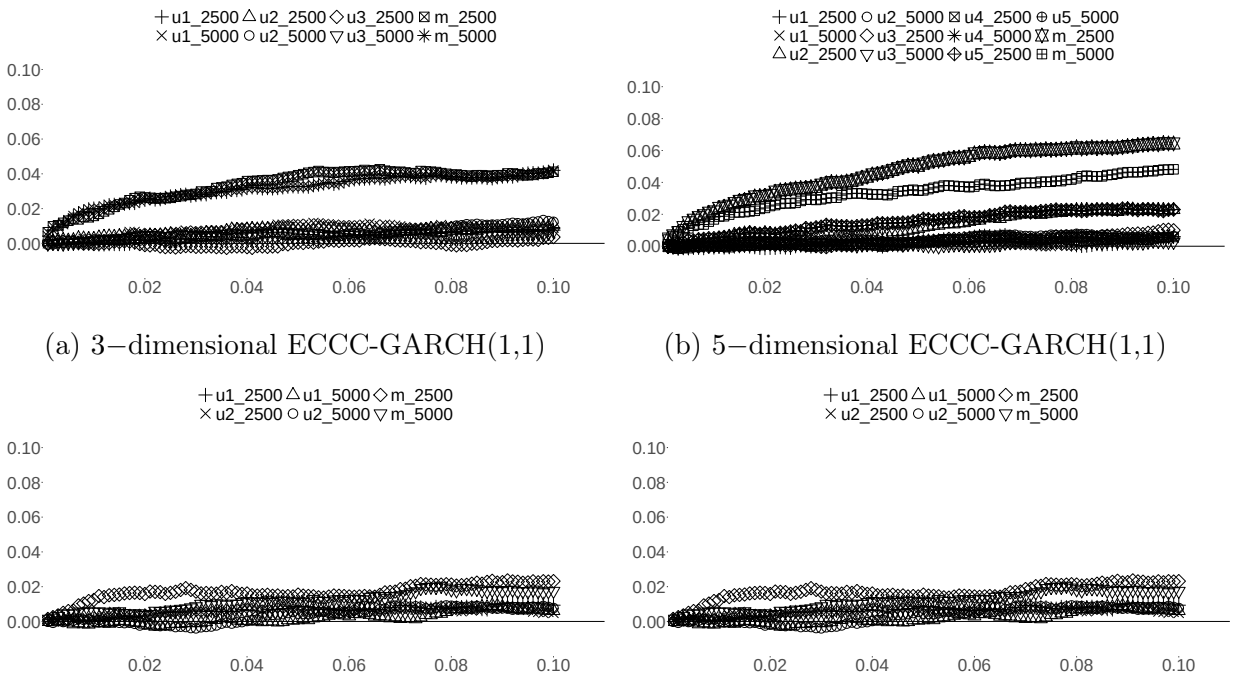

(a) 3−dimensional ECCC-GARCH(1,1)

(b) 5−dimensional ECCC-GARCH(1,1)

(c) ETVC-GARCH(1,1)

(d) EDCC-GARCH(1,1)

Figure 3: Size discrepancy plots for tests of parameter constancy in higher-dimensional ECCC-GARCH models (upper panels) and for artificial series generated from time-varying conditional correlations DGPs in Table 3 (lower panels). The size discrepancy is plotted against the nominal size. Results are shown for the univariate (ui_T), $i = 1, 2$, and multivariate robust (m_T) test statistics defined in (45) and (46), respectively, with $\widehat{\mathbf{x}}_{i1,t}$ and $\widehat{\mathbf{x}}_{i2,t}$ given in (56) and (56) for $T = 2500, 5000$. The number of replications for each simulation equals 5000.

6 Empirical application

In this section we illustrate the usefulness of the multivariate time-varying extended GARCH framework to sovereign bond markets. We employ daily data on 10-year government bond yields from October 3, 2005 until September 30, 2015 (2608 observations) to investigate volatility spillovers between sovereign bonds markets from Greece (GR), Ireland (IR) and Portugal (PT). The data were collected from the Thomson Reuters Datastream and transformed into continuously compounded rates of return. To avoid estimation problems, the observations in the series are truncated with a threshold of $+/-10$ standard deviations above/below extremely large returns. The aim is to investigate cross-market volatility transmissions and the dynamics of bond market co-movements during the global financial crisis and the European debt crisis. The daily 10-year government benchmark bond yields and their truncated returns are depicted in Figure 4. After the Greek deficit revision, Greece government bonds increased sharply, followed foremost by Portugal and Ireland. In fact, the Greek financial bailout in May 2010 was followed by the Irish bailout in November 2010 and the Portuguese bailout in April 2011. A closer look to the percent changes reveals an increasing pattern in the volatility on these European sovereign bond markets starting in late 2009. For the Irish series, the increase in volatility is more pronounced at the end of the sample period.

Table 4: Descriptive statistics of the daily government bond yield percent changes

	MIN.	MEAN	MAX.	S.D.	SK	KR	Q(5)	ARCH(5)
GREECE	−27.95	0.085	27.95	2.606	−0.592	28.96	16.28	40.08
					(0.000)	(0.000)	(0.006)	(0.000)
IRELAND	−19.09	−0.019	19.09	1.914	1.012	19.84	10.46	79.32
					(0.000)	(0.000)	(0.063)	(0.000)
PORTUGAL	−20.44	0.011	18.46	2.022	0.526	12.48	19.84	18.50
					(0.000)	(0.000)	(0.001)	(0.000)

Note: SK and KR denote, respectively, the excess kurtosis and skewness. Q(5) is the portmanteau test statistic for serial correlation of Francq and Zakoïan (2009) robust to the presence of ARCH effects up to order 5 and ARCH(5) is the test for ARCH effects of Engle (1982) up to order 5 (p-values in parentheses).

Summary statistics for the truncated series of yield percent changes can be found in Table 4. As expected, the bond yield returns exhibit a skewed and heavy-tailed distribution suggesting the series to be non-normally distributed. Results of the robust portmanteau

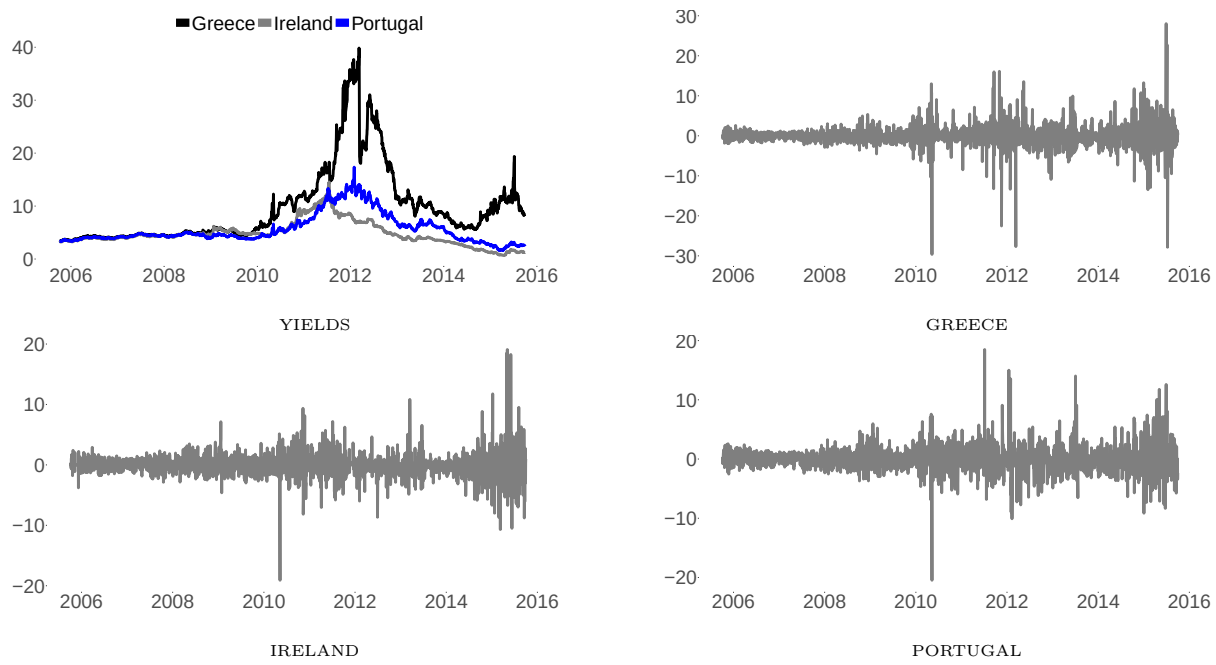

Figure 4: Daily 10-year government bond yields and truncated percent changes. The threshold for truncation is +/− 10 times the sample standard deviation.

Q(5) statistic of Francq and Zakoïan (2009) show time-dependence in the first moment for the Greek and Portuguese bond returns. To filter out the linear dependence we fit an AR(1) to the Greek bond returns and an ARMA(1,1) to the Portuguese bond returns. There is also evidence of higher-order ARCH effects in the bond returns from the results of the LM test of Engle (1982).

We apply the modelling strategy for the additive extended GARCH model and begin with the appropriate LM-type tests. First, we investigate the hypothesis that the ARCH and GARCH matrices are diagonal. The tests proposed by Nakatani and Teräsvirta (2009) and Pedersen (2017) are performed under the null hypothesis of no volatility spillovers. The results (not shown here but available upon request) strongly indicate the presence of volatility interactions as the p-values of the test statistics are smaller than 0.05. Next we turn out attention to testing parameter constancy against the extended additive time-dependent vector GARCH model. Robust versions of the univariate and multivariate test statistics for testing the constancy of volatility interactions are reported in Table 5. Results of the test statistics for the constancy of the full set of volatility parameters are shown in the upper panel. It is seen from the p-values that the null of constant parameters is strongly rejected by the univariate and multivariate test statistics suggesting that the volatility parameters

are time-varying and thereby providing support for the TV-ECC-GARCH model. In what follows, we attempt to disentangle changes in the dynamics of volatility (or co-volatility) by showing the parameter constancy test results in the standard GARCH coefficients and cross-market ARCH effects in the middle and lower panels of Table 5, respectively. The strong rejection of the parameter constancy hypothesis suggests structural changes in the standard GARCH coefficients and co-volatility processes during the observation period.

Specification of the TV-ECC-GARCH model includes determining the parameterisation of the transition function by choosing k_i. After parameter constancy is rejected, we attempt to identify the number of locations using the sequence of nested null hypothesis as discussed in subsection 4.3. Since the null hypothesis yielding the strongest rejection (measured by the p-value of the robust test) is H_{02i}, the rule is to select $k_i = 2$ for the Irish bond market. As for Greek and Portuguese returns, a single transition parameter suffices to capture the dominant changes in the volatility dynamics since the p-value of the test of H_{01i} is the smallest. For a more detailed discussion about this procedure see Teräsvirta (1994).

For fitting the TV-ECC-GARCH model we use the two-step approach of Francq and Zakoïan (2016) where the algorithm consists in estimating the individual conditional variances equation-by-equation and obtaining estimates of the conditional correlations specification in the second step. To obtain fully efficient estimates, the procedure must be repeated iteratively until convergence where the estimates are obtained by maximizing the full log-likelihood function. Compared to the two-step procedure, the multi-step approach yields more accurate estimates, but the computational burden is severely aggravated and the estimation problem becomes numerically more difficult. The two-step estimates of the model can be found in Table 6. The estimation results are broadly consistent with the results of the parameter constancy tests. The estimates as shown in the upper panel of Table 6 indicate there is evidence of structural changes in the volatility dynamics. We find an increasing trend in the baseline volatility for the three bond markets. Not surprisingly, the level of persistence increases from the low- to the high-volatility extreme state over time. This is precisely what one would expect moving from a tranquil to a turbulent period in the bond markets. The change in the volatility persistence is explained mostly by higher ARCH effects and smaller GARCH coefficients between the extreme states of volatility for Ireland and Portugal.

Table 5: Robust test statistics from the testing for parameter constancy in the univariate and multivariate forms for all parameters (upper panel), for the standard GARCH coefficients (middle panel) and for the cross-market ARCH coefficients (lower panel). The p-values are reported in parentheses.

	GREECE	IRELAND	PORTUGAL
H_{0i}: $\boldsymbol{\varphi}_{i3} = \boldsymbol{\varphi}_{i2} = \boldsymbol{\varphi}_{i1} = \mathbf{0}_5$	33.72 (0.004)	40.35 (0.000)	29.83 (0.013)
H_{03i}: $\boldsymbol{\varphi}_{i3} = \mathbf{0}_5$	8.043 (0.154)	3.988 (0.551)	6.281 (0.280)
H_{02i}: $\boldsymbol{\varphi}_{i2} = \mathbf{0}_5 \vert \boldsymbol{\varphi}_{i3} = \mathbf{0}_5$	2.618 (0.759)	17.53 (0.004)	1.962 (0.854)
H_{01i}: $\boldsymbol{\varphi}_{i1} = \mathbf{0}_5 \vert \boldsymbol{\varphi}_{i3} = \boldsymbol{\varphi}_{i2} = \mathbf{0}_5$	13.32 (0.021)	7.102 (0.213)	15.64 (0.008)
H_0: $\boldsymbol{\varphi}_1 = (\boldsymbol{\varphi}'_{\mathrm{GR},1}, \boldsymbol{\varphi}'_{\mathrm{IR},1}, \boldsymbol{\varphi}'_{\mathrm{PT},1})' = \mathbf{0}_{15}$		36.06 (0.002)	
$\mathsf{H}_{0i,1}$: $\boldsymbol{\varphi}_{i3,1} = \boldsymbol{\varphi}_{i2,1} = \boldsymbol{\varphi}_{i1,1} = \mathbf{0}_3$	30.35 (0.000)	25.33 (0.003)	15.85 (0.051)
$\mathsf{H}_{03i,1}$: $\boldsymbol{\varphi}_{i3,1} = \mathbf{0}_3$	5.467 (0.141)	3.256 (0.354)	3.473 (0.324)
$\mathsf{H}_{02i,1}$: $\boldsymbol{\varphi}_{i2,1} = \mathbf{0}_3 \vert \boldsymbol{\varphi}_{i3,1} = \mathbf{0}_3$	1.327 (0.723)	11.76 (0.008)	1.388 (0.708)
$\mathsf{H}_{01i,1}$: $\boldsymbol{\varphi}_{i1,1} = \mathbf{0}_3 \vert \boldsymbol{\varphi}_{i3,1} = \boldsymbol{\varphi}_{i2,1} = \mathbf{0}_3$	9.396 (0.024)	6.926 (0.074)	11.56 (0.009)
$\mathsf{H}_{0i,2}$: $\boldsymbol{\varphi}_{i3,2} = \boldsymbol{\varphi}_{i2,2} = \boldsymbol{\varphi}_{i1,2} = \mathbf{0}_2$	24.66 (0.000)	9.287 (0.158)	19.27 (0.004)
$\mathsf{H}_{03i,2}$: $\boldsymbol{\varphi}_{i3,2} = \mathbf{0}_2$	3.236 (0.198)	3.361 (0.186)	1.406 (0.495)
$\mathsf{H}_{02i,2}$: $\boldsymbol{\varphi}_{i2,2} = \mathbf{0}_2 \vert \boldsymbol{\varphi}_{i3,2} = \mathbf{0}_2$	4.304 (0.116)	6.338 (0.042)	6.446 (0.040)
$\mathsf{H}_{01i,2}$: $\boldsymbol{\varphi}_{i1,2} = \mathbf{0}_2 \vert \boldsymbol{\varphi}_{i3,2} = \boldsymbol{\varphi}_{i2,2} = \mathbf{0}_2$	8.784 (0.012)	0.735 (0.692)	3.849 (0.146)

The off-diagonal elements of the estimated ARCH matrix for each extreme volatility state are reported in Table 6. The results suggest that the bidirectional cross-market volatility effects between the Portuguese and Greek sovereign bonds changed over time. In other words, the effect of shocks to the Portuguese bond on the volatility of the Greek bond increased significantly after October 2009. Conversely, we observe that the effect of shocks to the Greek bond on the volatility of the Portuguese bond is notably larger before January 2011. The effects on the Irish bond volatility from shocks to the Greek bond seem to be stronger before March 2010 and after April 2015. When the shock occurs to the Portuguese bond, the effects on the Irish bond volatility are significantly higher between March 2010 and April 2015. Our results suggest higher effects on the Portuguese sovereign bond volatility after January 2011 from shocks to the Irish bond. Overall, volatility interactions appear to be stronger during the most acute phase of the European sovereign debt crisis. Our findings suggest that volatility-based contagion is identified bidirectionally for the pairwise Greece−Portugal and Ireland−Portugal, and unidirectionally from Greece to Ireland.

In the lower panel of Table 6 are reported the estimated transition parameters. The slope estimates yield smooth changes between the extreme states of volatility as depicted in Figure 5. From the results, a single transition seems to be sufficient to capture the dominant changes in the volatilities of the Greek and Portuguese markets whereas two major structural changes can be identified in the Irish bond market. By looking at the locations of transition, the mid-point of change[1] occurs in October 2009 for the Greek sovereign bond market and in January 2011 for the Portuguese sovereign bond, few months before its financial request. With respect to the Irish sovereign bond, the first and second structural changes occur, respectively, in March 2010 and April 2015.

A closer look to the estimated volatilities of the sovereign bond returns in Figure 6 shows an increasing trend following the Greek deficit revision (marked by the red dotted line) which is particularly remarkable for Ireland and Portugal by the end of the sample period. The results further suggest that the ARCH effects are assumed to be constant, the impact of larger shocks tends to be underestimated by the ECCC-GARCH model. Therefore, constant

[1]For a general transition function, the transition may be already half-completed at c if γ is small. When the speed of transition is very high, it has no implication for defining the phases of transition using the estimated locations.

Table 6: Estimation results (standard errors in parentheses) for the variance equations (upper panel) and transition functions (lower panel) of the TV-ECC-GARCH(1, 1) model in the extreme states.

	STATE I				STATE II		
	GREECE	IRELAND	PORTUGAL		GREECE	IRELAND	PORTUGAL
$\hat{\boldsymbol{\omega}}$	0.117 (0.042)	0.012 (0.007)	0.001 (0.008)	$\hat{\boldsymbol{\omega}} + \hat{\boldsymbol{\omega}}^*$	0.609 (0.059)	0.053 (0.036)	0.131 (0.043)
$\hat{\mathbf{A}}_1$	0.091 (0.034)	0.006 (0.015)	0.000 (0.028)	$\hat{\mathbf{A}}_1 + \hat{\mathbf{A}}_1^*$	0.243 (0.013)	0.000 (0.006)	0.015 (0.007)
	0.023 (0.011)	0.000 (0.017)	0.013 (0.016)		0.000 (0.013)	0.211 (0.149)	0.034 (0.014)
	0.040 (0.011)	0.000 (0.008)	0.008 (0.015)		0.002 (0.004)	0.020 (0.008)	0.032 (0.009)
$\hat{\mathbf{B}}_1$	0.702 (0.080)			$\hat{\mathbf{B}}_1 + \hat{\mathbf{B}}_1^*$	0.742 (0.011)		
		0.947 (0.016)				0.755 (0.133)	
			0.944 (0.012)				0.924 (0.014)

	GREECE	IRELAND	PORTUGAL
$\hat{\gamma}_i$	12.76 (1.773)	15.49 (12.91)	6.962 (2.233)
$\hat{c}_{i1}$	0.400 (0.032)	0.441 (0.205)	0.529 (0.084)
	Oct 2009	Mar 2010	Jan 2011
$\hat{c}_{i2}$		0.954 (0.178)	
		Apr 2015	

volatility interactions may be insufficient to capture all the variation in the daily volatilities during periods of market distress. This result is especially notable for the volatility processes of the Greek and Irish sovereign bonds. For smaller shocks and calm periods, the estimated volatility processes from the TV-ECC-GARCH and ECCC-GARCH models remain very close. Extending the specification by allowing cross effects between markets does improve the model fit to the data according to model selection by the Bayesian information criterion. Accounting for nonstationarity in the volatility equations leads to further improvement in the estimation of the model as persistence is notably reduced and the information criteria is minimized by fitting the TV-ECC-GARCH model.

Test results associated with the hypothesis of constant conditional correlations strongly reject the null hypothesis against the alternative of dynamic conditional correlations and smoothly time-varying correlations. Results are not shown, but they are available upon request. For more details on the tests, we refer to Engle (2002) and Silvennoinen and Teräsvirta (2005, 2015). The estimated results for different correlation structures are visible

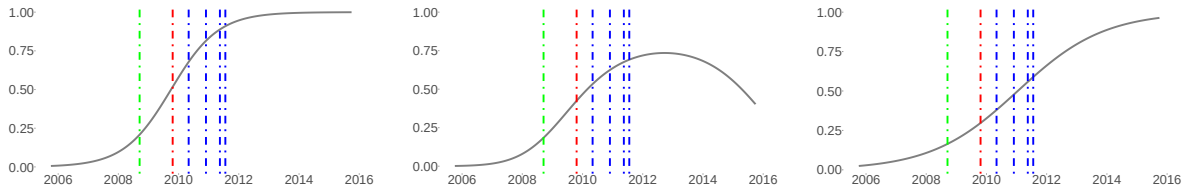

(a) GREECE (b) IRELAND (c) PORTUGAL

Figure 5: Estimated transition functions for the Greek, Irish and Portuguese sovereign bond returns. The dashed vertical lines indicate the dates of the Lehman Brothers bankruptcy (green line), the Greek deficit revision (red line) and the first Greek financial bailout in May 2010, the Irish bailout in November 2010, the Portuguese bailout in May 2011 and the second Greek bailout in July 2011 (blue line).

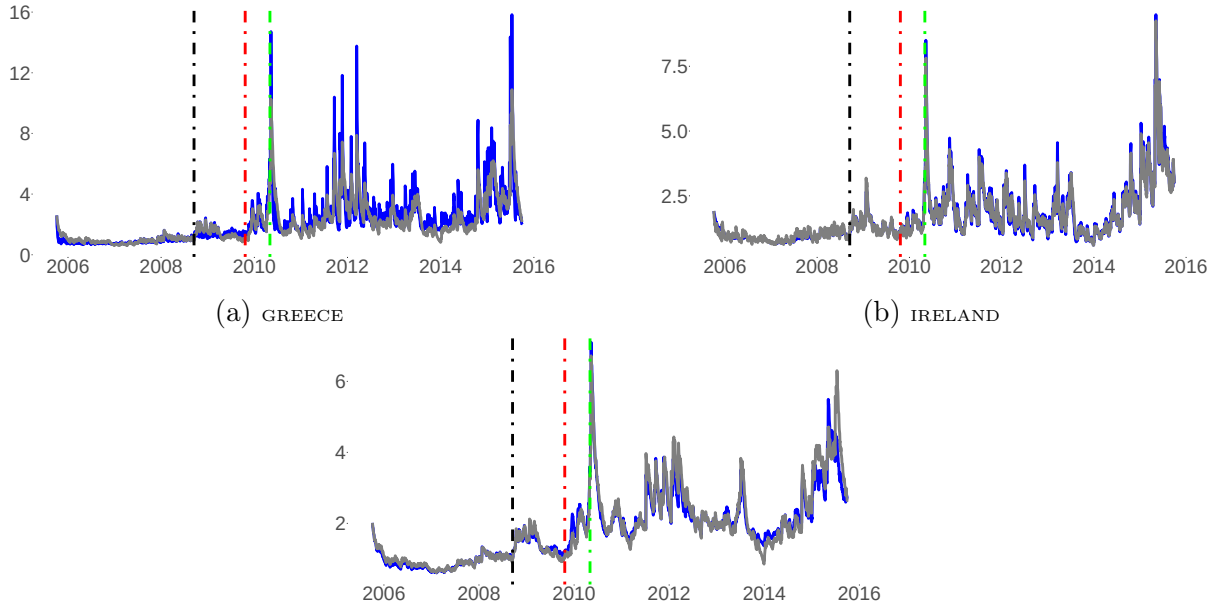

(a) GREECE (b) IRELAND

(c) PORTUGAL

Figure 6: Estimated conditional volatilities for the Greek, Irish and Portuguese sovereign bonds from the TV-ECC-GARCH(1, 1) model (blue curve) and ECCC-GARCH(1, 1) model (grey curve). The dashed vertical lines indicate the dates of the Lehman Brothers bankruptcy (black line), the Greek deficit revision (red line) and the first Greek financial bailout (green line).

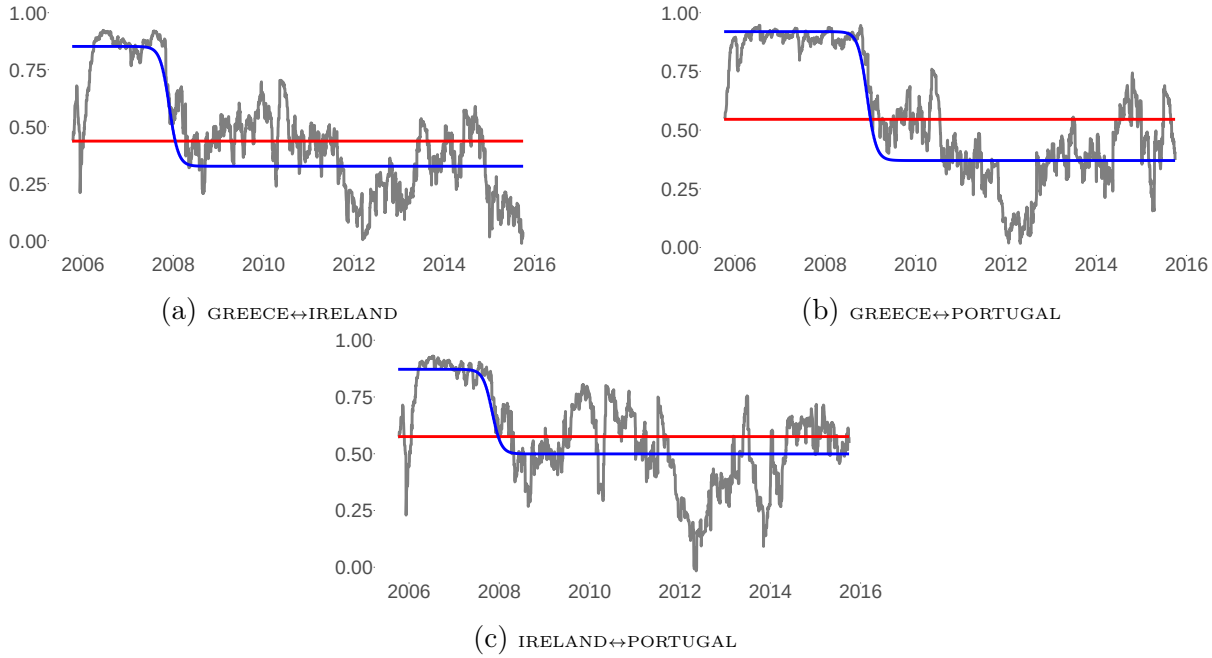

(a) GREECE↔IRELAND (b) GREECE↔PORTUGAL

(c) IRELAND↔PORTUGAL

Figure 7: Estimated bivariate dynamic conditional correlations (grey line) from the TV-EDCC-GARCH(1,1) model, time-varying unconditional correlations (blue line) from the TV-ETVC-GARCH(1,1) model and constant conditional correlations (red line) from the TV-ECC-GARCH(1,1) model.

in Figure 7. We choose estimating the bivariate models over the 3-dimensional model in order to obtain more precise estimates for the transition parameters in the TV-ETVC-GARCH(1,1) model. The estimation results have interesting interpretations. We observe that the short-run dynamic correlations obtained from the TV-EDCC-GARCH(1,1) model tend to fluctuate around the time-varying unconditional correlations estimated from the TV-ETVC-GARCH(1,1) model. The time-varying (un)conditional correlations show a decreasing trend over time suggesting that the co-movements of the yield returns become weaker during the period of higher uncertainty. The long-term time-varying correlations show a downward trend movement descending to a level lower than that of before the global and sovereign debt crises and turn out to become smaller than "normal" market co-movements proxied by the constant conditional correlations[1].

[1]As the level of market interdependence, the normal comovement that is observed during both calm and turbulent periods, we use the estimated constant conditional correlation for the total sample period; see Martins and Amado (2018)).

7 Conclusions

In this paper we propose an additive structure for the extended vector GARCH process to investigate the dynamics of co-dependence volatility across financial markets. In this regard, we consider the general class of conditional correlation GARCH models where the volatility parameters are allowed to change smoothly over time by adding a deterministic time-dependent component to the variance equations. Within our approach, the timing of volatility regime changes is identified from a purely data-driven procedure.

For detecting changes in the volatility and co-volatility spillovers, we develop a Lagrange multiplier test for testing the hypothesis of parameter constancy where the rejection of the null hypothesis provides evidence for structural changes in the (co-)volatility processes. Crisis-contingent structural changes in the volatility interactions can be interpreted as cross-market contagion, thereby the new test can be regarded as a volatility-based test of contagion. Simulation experiments show that the robust univariate LM-type version of the test to departures from normality is reasonably well-behaved in finite samples.

Our modelling technique is applied to Greek, Irish and Portuguese sovereign bond returns and we find the new statistical test to be an useful tool in model specification for the extended vector GARCH model. Results indicate a strong rejection of the parameter constancy hypothesis suggesting structural changes in the standard GARCH coefficients and co-volatility processes during the observation period. Once the model accounts for time-variation in the volatility interactions, the fit of the model substantially improves and the evidence for volatility persistence is remarkably decreased. The computational burden of the higher-dimensional model is alleviated by estimating the conditional variances equation-by-equation for each individual series in the first step and the correlation matrix in the second step. Our estimation results further suggest that volatility interactions seem to be stronger during the most acute phase of the European sovereign debt crisis. Volatility-based contagion is also identified bidirectionally for the pairwise Greece-Portugal and Ireland-Portugal, and unidirectionally from Greece to Ireland.

Albeit the tests for structural changes in the dynamics of volatility (or co-volatility) seem rather robust against time-varying conditional correlations, it would be of interest to extend these tests to cover the extended conditional correlation GARCH model with time-varying

correlations. Another interesting practical question would be to investigate how volatility responds to negative and positive shocks within this framework. A possible extension to the model would be to include the so-called leverage effect as in Francq and Zakoïan (2012), but since empirical evidence is scanty in response of conditional volatility to the sign of shocks for bond returns (Cappiello et al. (2006)), the effects of asymmetric volatility shocks were not considered in this work. Such issues, however, are left for future research.

Acknowledgements

The financial support provided by the Portuguese Foundation for Science and Technology under the Doctoral scholarship SFRH/BD/109539/2015 is acknowledged. This research has also been supported by funding from COMPETE (Ref. No. POCI-01-0145-FEDER-028234), with the FCT/MEC's financial support through national funding and by the ERDF through the Operational Programme on "Competitiveness and Internationalization" - COMPETE 2020 under the PT2020 Partnership Agreement. Part of the work for this paper was carried out while the first author was visiting the Queen Mary University of London, and during the second author's visit to Rady School of Management at the University of California San Diego. Kind hospitality is gratefully acknowledged at both institutions. Material from this paper has been presented at the One Day Meeting on Statistics and Applied Probability, Guimarães, Portugal, October 2019; North American Summer Meeting of the Econometric Society, Davis, June 2018; Conference on New Trends and Developments in Econometrics, Lisbon, June 2018; 1st International Conference in Quantitative Finance and Financial Econometrics, Marseille, May 2018; Conference on Portfolio Managing, Stochastic Processes and Financial Econometrics, Florence, May 2018; 8th International Conference on Mathematical and Statistical Methods for Actuarial Sciences and Finance, Madrid, April 2018; XIX Quantitative Finance Workshop, Rome, January 2018; 11th International Conference on Computational and Financial Econometrics, London, December 2017; 28th European Conference of the Econometrics Community, Amsterdam, December 2017; and in seminars at University of Surrey, March 2021; University of California Riverside, October 2019; University of Florence, Florence, May 2018; University of Minho, Braga, November

2017; and Scuola Normale Superiore, Pisa, February 2017. The authors would like to thank participants at these occasions for their comments and Marcelo Fernandes for useful discussions and suggestions.

References

Baillie, R. T. and Bollerslev, T.: 1990, Intra-day and inter-market volatility in foreign exchange rates, *Review of Economic Studies* **58**, 565–585.

Bauwens, L., Laurent, S. and Rombouts, J. V. K.: 2006, Multivariate GARCH models: A survey, *Journal of Applied Econometrics* **21**, 79–109.

Bollerslev, T.: 1990, Modelling the coherence in short-run nominal exchange rates: A multivariate generalized ARCH model, *Review of Economics and Statistics* **72**, 498–505.

Cappiello, L., Engle, R. F. and Sheppard, K.: 2006, Asymmetric dynamics in the correlations of global equity and bond returns, *Journal of Financial Econometrics* **4**, 537–572.

Cheung, Y.-W. and Ng, L. K.: 1996, A causality-in-variance test and its application to financial market prices, *Journal of Econometrics* **72**, 33–48.

Chiang, M.-H. and Wang, L.-M.: 2011, Volatility contagion: A range-based volatility approach, *Journal of Econometrics* **165**, 175–189.

Cifarelli, G. and Paladino, G.: 2005, Volatility linkages across three major equity markets: A financial arbitrage approach, *Journal of International Money and Finance* **24**, 413–439.

Conrad, C. and Karanasos, M.: 2010, Negative volatility spillovers in the unrestricted ECCC-GARCH model, *Econometric Theory* **26**, 838–862.

Dahlhaus, R. and Rao, S. S.: 2006, Statistical inference for time-varying ARCH processes, *The Annals of Statistics* **34**, 1075 – 1114.

Diebold, F. X. and Yilmaz, K.: 2009, Measuring financial asset return and volatility spillovers, with application to global equity markets, *The Economic Journal* **119**, 158–171.

Engle, R. F.: 1982, Autoregressive conditional heteroskedasticity with estimates of the variance of United Kingdom inflation, *Econometrica* **50**, 987–1007.

Engle, R. F.: 2002, Dynamic conditional correlation: A simple class of multivariate generalized autoregressive conditional heteroskedasticity models, *Journal of Business & Economic Statistics* **20**, 339–350.

Engle, R. F. and Susmel, R.: 1993, Common volatility in international equity markets, *Journal of Business & Economic Statistics* **11**, 167–176.

Forbes, K. J. and Rigobon, R.: 2002, No contagion, only interdependence: Measuring stock market comovements, *The Journal of Finance* **57**, 2223–2261.

Francq, C. and Zakoïan, J.-M.: 2009, Bartlett's formula for a general class of nonlinear processes, *Journal of Time Series Analysis* **30**, 449–465.

Francq, C. and Zakoïan, J.-M.: 2012, QML estimation of a class of multivariate asymmetric GARCH models, *Econometric Theory* **28**, 179–206.

Francq, C. and Zakoïan, J.-M.: 2016, Estimating multivariate volatility models equation by equation, *Journal of the Royal Statistical Society Series B (Statistical Methodology)* **78**, 613–635.

Granger, C. W. J.: 1993, Strategies for modelling nonlinear time-series relationships, *Economic Record* **69**, 233–239.

Hamao, Y., Masulis, R. W. and Ng, V.: 1990, Correlations in price changes and volatility across international stock markets, *The Review of Financial Studies* **3**, 281–307.

He, C. and Teräsvirta, T.: 2004, An extended constant conditional correlation GARCH model and its fourth-moment structure, *Econometric Theory* **20**, 904–926.

Hong, Y.: 2001, A test for volatility spillover with application to exchange rates, *Journal of Econometrics* **103**, 183âĂŞ224.

Jeantheau, T.: 1998, Strong consistency of estimators for multivariate ARCH models, *Econometric Theory* **14**, 70–86.

Jung, R. and Maderitsch, R.: 2014, Structural breaks in volatility spillovers between international financial markets: Contagion or mere interdependence?, *Journal of Banking & Finance* **47**, 331–342.

Karanasos, M., Ali, F. M., Margaronis, Z. and Nath, R.: 2018, Modelling time varying volatility spillovers and conditional correlations across commodity metal futures, *International Review of Financial Analysis* **57**, 246–256.

Karanasos, M., Paraskevopoulos, A. G., Ali, F. M., Karoglou, M. and Yfanti, S.: 2014, Modelling stock volatilities during financial crises: A time varying coefficient approach, *Journal of Empirical Finance* **29**, 113–128.

King, M. A. and Wadhwani, S.: 1990, Transmission of volatility between stock markets, *Review of Financial Studies* **3**, 5–33.

Leung, H., Schiereck, D. and Schroeder, F.: 2017, Volatility spillovers and determinants of contagion: Exchange rate and equity markets during crises, *Economic Modelling* **61**, 169–180.

Lin, C.-F. J. and Teräsvirta, T.: 1994, Testing the constancy of regression parameters against continuous structural change, *Journal of Econometrics* **62**, 211–228.

Lin, W.-L., Engle, R. F. and Ito, T.: 1994, Do bulls and bears move across borders? International transmission of stock returns and volatility, *The Review of Financial Studies* **7**, 507–538.

Ling, S. and McAleer, M.: 2003, Asymptotic theory for a vector ARMA-GARCH model, *Econometric Theory* **19**, 280–310.

Liu, T. and Gong, X.: 2020, Analyzing time-varying volatility spillovers between the crude oil markets using a new method, *Energy Economics* **87**, 104711.

Luukkonen, R., Saikkonen, P. and Teräsvirta, T.: 1988, Testing linearity against smooth transition autoregressive models, *Biometrika* **75**, 491–499.

Martins, S. and Amado, C.: 2018, Financial market contagion and the sovereign debt crisis: A smooth transition approach. NIPE − WP 08/2018. Available at http://www.nipe.eeg.uminho.pt/Uploads/WP_2018/NIPE_WP_8_2018.pdf.

Nakatani, T. and Teräsvirta, T.: 2009, Testing for volatility interactions in the constant conditional correlation GARCH model, *Econometrics Journal* **12**, 147–163.

Pedersen, R. S.: 2017, Inference and testing on the boundary in extended constant conditional correlation GARCH models, *Journal of Econometrics* **196**, 23–36.

R Core Team: 2017, R: A language and environment for statistical computing. Available at https://www.R-project.org.

Silvennoinen, A. and Teräsvirta, T.: 2005, Multivariate autoregressive conditional heteroskedasticity with smooth transitions in conditional correlations. SSE/EFI Working Paper Series in Economics and Finance No. 577.

Silvennoinen, A. and Teräsvirta, T.: 2009, Multivariate GARCH models., *in* T. Mikosch, J.-P. Kreiß, R. A. Davis and T. G. Andersen (eds), *Handbook of Financial Time Series*, Springer Berlin Heidelberg, Berlin, Heidelberg, pp. 201–229.

Silvennoinen, A. and Teräsvirta, T.: 2015, Modeling conditional correlations of asset returns: A smooth transition approach, *Econometric Reviews* **34**, 174–197.

Silvennoinen, A. and Teräsvirta, T.: 2017, Consistency and asymptotic normality of maximum likelihood estimators of a multiplicative time-varying smooth transition correlation GARCH model. CREATES Research Paper 2017−28.

Teräsvirta, T.: 1994, Specification, estimation, and evaluation of smooth transition autoregressive models, *Journal of the American Statistical Association* **89**, 208–218.

Teräsvirta, T.: 1998a, Modeling economic relationships with smooth transition regressions, *in* A. Ullah and D. Giles (eds), *Handbook of Applied Economic Statistics*, Dekker, New York.

Teräsvirta, T.: 1998b, Modeling economic relationships with smooth transition regressions, *in* A. Ullah and D. Giles (eds), *Handbook of Applied Economic Statistics*, New York: Dekker, Berlin, Heidelberg, pp. 507–552.

Teräsvirta, T., Tjøstheim, D. and Granger, C. W. J.: 2010, Modelling nonlinear economic time series, Oxford University Press, Oxford.

Tse, Y. K. and Tsui, A. K. C.: 2002, A multivariate generalized autoregressive conditional heteroscedasticity model with time-varying correlations, *Journal of Business & Economic Statistics* **20**, 351–362.

Wooldridge, J. M.: 1990, A unified approach to robust, regression-based specification tests, *Econometric Theory* **6**, 17–43.

Wooldridge, J. M.: 1991, On the application of robust, regression-based diagnostics to models of conditional means and conditional variances, *Journal of Econometrics* **47**, 5–46.

Most Recent Working Paper

NIPE WP 12/2021	**Campos-Martins, S.**, and **Amado, C.**, Modelling Time-Varying Volatility Interactions, 2021
NIPE WP 11/2021	Brekke, K. R., Siciliani, L. and **Straume, O. R.**, Competition, quality and integrated health care, 2021
NIPE WP 10/2021	Felipe, I. J. S., Mendes-Da-Silva, W., **Leal, C. C.**, and Santos, D. B., Reward Crowdfunding Campaigns: Time-To-Success Analysis, 2021
NIPE WP 9/2021	**Fernando Alexandre,** Avaliação dos incentivos financeiros às empresas em Portugal: QREN (2007-2013) e PT2020 (2014-2018), 2021
NIPE WP 8/2021	**Rosa-Branca Esteves**, Can personalized pricing be a winning strategy in oligopolistic markets with heterogeneous demand customers? Yes, it can, 2021
NIPE WP 7/2021	**Loureiro, G.,** and **Silva, S.**, The Impact of Securities Regulation on the Information Environment around Stock-Financed Acquisitions, 2021
NIPE WP 6/2021	**Aguiar-Conraria, L.**, Conceição, G., and **Soares, M. J.**, How far is gas from becoming a global commodity?, 2021
NIPE WP 5/2021	**Rosa-Branca Esteves** and **Francisco Carballo Cruz**, Access to Data for Personalized Pricing: Can it raise entry barriers and abuse of dominance concerns?, 2021
NIPE WP 4/2021	**Rosa-Branca Esteves**, Liu, Q. and Shuai, J. Behavior-Based Price Discrimination with Non-Uniform Distribution of Consumer Preferences, 2021
NIPE WP 3/2021	**Ghandour, Z.,** Siciliani, L. and **Odd Rune Straume**, Investment and Quality Competition in Healthcare Markets, 2021
NIPE WP 2/2021	**Martins, João**, **Linda Veiga and** Bruno **Fernandes**, Does electronic government deter corruption? Evidence from across the world, 2021
NIPE WP 1/2021	Kurt R. Brekke, Dag Morten Dalen and **Odd Rune Straume**, Paying for pharmaceuticals: uniform pricing versus two-part tariffs, 2021
NIPE WP 10/2020	**Ghandour, Z.** and **Odd Rune Straume**, Quality competition in mixed oligopoly, 2020
NIPE WP 09/2020	Gabrielsen, T. S., Johansen, B. O., and **Odd Rune Straume**, National pricing with local quality competition, 2020
NIPE WP 08/2020	Engle, R. F., and **Campos-Martins, S.**, Measuring and Hedging Geopolitical Risk, 2020
NIPE WP 07/2020	Boukari, M., and **Veiga, F. J.**, Fiscal Forecast Manipulations and Electoral Results: Evidence from Portuguese Municipalities, 2020
NIPE WP 06/2020	**Alexandre, F., Cruz, S**. and **Portela, M.**, Financial distress and the role of management in micro and small-sized firms, 2020
NIPE WP 05/2020	Cooke, D., Ana P. Fernandes and **Priscila Ferreira**, Entry Deregulation, Firm Organization and Wage Inequality, 2020
NIPE WP 04/2020	**Fernando Alexandre**, Pedro Bação, **João Cerejeira**, **Hélder Costa** and **Miguel Portela**, Minimum wage and financially distressed firms: another one bites the dust, 2020
NIPE WP 03/2020	**Luís Sá** and **Odd Rune Straume**, Quality provision in hospital markets with demand inertia: The role of patient expectations, 2020
NIPE WP 02/2020	**Rosa-Branca Esteves**, Liu Qihong and Shuai, J., Behavior-Based Price Discrimination with Non-Uniform Distribution of Consumer Preferences, 2020
NIPE WP 01/2020	Diogo Teixeira and **J. Cadima Ribeiro,** "Residents' perceptions of the tourism impacts on a mature destination: the case of Madeira Island", 2020
NIPE WP 17/2019	Liao, R. C., **Loureiro, G.**, and Taboada, A. G., "Women on Bank Boards: Evidence from Gender Quotas around the World", 2019
NIPE WP 16/2019	**Luís Sá,** "Hospital Competition Under Patient Inertia: Do Switching Costs Stimulate Quality Provision?", 2019
NIPE WP 15/2019	**João Martins** and **Linda G. Veiga**, "Undergraduate students' economic literacy, knowledge of the country's economic performance and opinions regarding appropriate economic policies", 2019
NIPE WP 14/2019	**Natália P. Monteiro, Odd Rune Straume** and **Marieta Valente,** "Does remote work improve or impair firm labour productivity? Longitudinal evidence from Portugal", 2019